

Glucose-Responsive Microparticle-Loaded Dissolving Microneedles for Selective Delivery of Metformin: A Proof-of-Concept Study

Nur Syafika, Sumayya Binti Abdul Azis, Cindy Kristina Enggi, Hanin Azka Qonita, Tiara Resky Anugrah Mahmud, Ahmad Abizart, Rangga Meidianto Asri, and Andi Dian Permana*



Cite This: *Mol. Pharmaceutics* 2023, 20, 1269–1284



Read Online

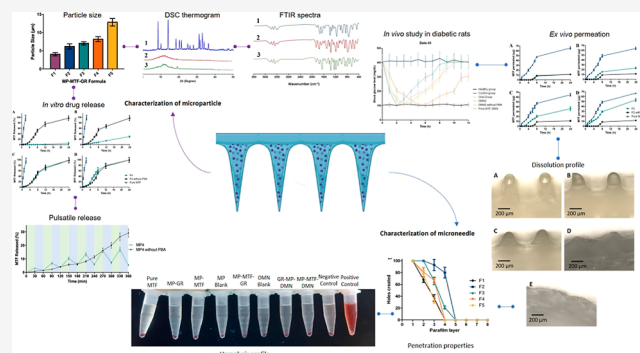
ACCESS |

Metrics & More

Article Recommendations

ABSTRACT: Diabetes mellitus (DM) is a metabolic disorder that is one of the most common health problems in the world, primarily type 2 DM (T2DM). Metformin (MTF), as the first-line treatment of DM, is effective in lowering glucose levels, but its oral administration causes problems, including gastrointestinal side effects, low bioavailability, and the risk of hypoglycemia. In this study, we formulated MTF into microparticles incorporating a glucose-responsive polymer (MP–MTF–GR), which could potentially increase the bioavailability and extend and control the release of MTF according to glucose levels. This system was delivered by dissolving microneedles (MP–MTF–GR–DMN), applied through the skin, thereby preventing gastrointestinal side effects of orally administered MTF. MP–MTF–GR was formulated using various concentrations of gelatin as a polymer combined with phenylboronic acid (PBA) as a glucose-responsive material. MP–MTF–GR was encapsulated in DMN using polyvinyl pyrrolidone (PVP) and polyvinyl alcohol (PVA) as DMN polymers. The physicochemical evaluation of MP–MTF–GR showed that MTF could be completely entrapped in MP with the percentage of MTF trapped increasing with increasing gelatin concentration without changing the chemical structure of MTF and producing stable MP. In addition, the results of the physicochemical evaluation of MP–MTF–GR–DMN showed that DMN had adequate mechanical strength properties and penetration ability and was stable to environmental changes. The results of the *in vitro* release and *ex vivo* permeation study on media with various concentrations of glucose showed that the release and permeation of MTF from the formula increased with increasing glucose levels in the media. The MP–MTF–GR–DMN formula successfully delivered MTF through the skin at 11.30 ± 0.29 , 23.31 ± 1.64 , 36.12 ± 3.77 , and $53.09 \pm 3.01 \mu\text{g}$ from PBS, PBS + glucose 1%, PBS + glucose 2%, and PBS + glucose 4%, respectively, at 24 h, which indicates glucose-responsive permeation and release behavior. The formula developed was also proven to be nontoxic based on hemolysis tests. Importantly, the *in vivo* study on the rat model showed that this combination approach could provide a better glucose reduction compared to other routes, reducing the blood glucose level to normal levels after 3 h and maintaining this level for 8 h. Furthermore, this approach did not change the skin moisture of the rats. This MP–MTF–GR–DMN is a promising alternative to MTF delivery to overcome MTF problems and increase the effectiveness of T2DM therapy.

KEYWORDS: metformin, glucose response, microparticle, dissolving microneedle, transdermal delivery



1. INTRODUCTION

Diabetes mellitus (DM) is a chronic metabolic disorder characterized by elevated blood glucose levels (BGLs). The cases of DM are increasing in recent years. Data from the International Diabetes Foundation (IDF) shows that in 2021, there were 536.6 million people with DM worldwide, and it is estimated to go up to 643 and 783 million by 2030 and 2045, respectively. More than 90% of these cases are type 2 DM (T2DM).¹

The first-line treatment of T2DM is metformin (MTF), a biguanide antihyperglycemic agent. More than 120 million people with DM use MTF for their treatment. MTF is

currently available in the form of tablets, modified tablets, capsules, suspensions, and solutions, which is administered orally.² The safety and efficacy of MTF in lowering BGLs have been proven.^{2,3} The previous meta-analysis showed that MTF could reduce HbA1c (glycated hemoglobin) levels by about

Received: November 6, 2022

Revised: January 11, 2023

Accepted: January 11, 2023

Published: January 20, 2023



1.5–2.0% and fasting blood glucose (FBG) (fasting blood sugar) by about 50–70 mg/dL.² MTF can reduce BGLs by inhibiting hepatic gluconeogenesis, reducing glucose absorption in the intestine, and increasing glucose uptake in tissues.^{3–5} MTF can reduce adenosine triphosphate (ATP) and increase adenosine monophosphate (AMP) by reducing mitochondrial complex I activity. Hence, MTF causes the activation of AMP-activated protein kinase (AMPK), an enzyme that plays an important role in regulating energy metabolism. Activated AMPK will inhibit gluconeogenesis in the liver and increase fatty acid oxidation, thereby lowering BGLs.^{4,6}

In addition, MTF also works to reduce glucose levels through its activity in the intestines. Unfortunately, this site action of MTF is also the site that results in adverse effects. MTF can increase glucose uptake and glucose metabolism through anaerobic metabolism in the intestine. This mechanism produces lactic acid in enterocytes, which is then transported to the liver, which causes lactic acidosis.^{5,7,8} About 1–3 per 30,000 MTF users are found to have lactic acidosis yearly.^{4,6} MTF can change the microbiome in the gut, which causes an increase in GLP-1, thereby increasing the regulation of glucose levels.^{4,5,7,8} However, changes in the microbiome also lead to increased production of lactic acid and decreased absorption of bile acids. This mechanism causes diarrhea and other gastrointestinal side effects, including nausea, vomiting, constipation, stomach pain and cramps, and flatulence.^{5,7,8} Some studies reported that 20–30% of patients treated with MTF experienced gastrointestinal effects that led to intolerance and 5% of them could not continue treatment or needed a dose adjustment.^{2,4}

Although the number of cases of hypoglycemia with MTF is lesser than with the use of sulfonylureas and insulin, there are still cases of hypoglycemia. A previous study showed 112 cases of hypoglycemia from 4072 cases of MTF overdose.^{9,10} This risk of hypoglycemia can occur because of the long-term and undisciplined administration of MTF. The other limitation of MTF in the treatment of T2DM is the varying absorption profile. MTF has a bioavailability of about 50–60%, which can change according to food intake. Its bioavailability will increase in the fasting state and decrease with the intake of high-fat foods. This causes the amount of MTF absorbed to be different and affects the resulting therapeutic effect as well.^{5,8}

MTF delivery via the transdermal route can be an alternative to overcome these problems. Previously, transdermal delivery of MTF has been developed through a hydrogel-forming microneedle (MN) system.⁵ This system can be an alternative to transdermal delivery. Its permeation was significantly increased compared to pure MTF. MNs via transdermal delivery have many advantages but still have some limitations. Drugs released from MN result in uncontrolled release behavior and do not demand physiological changes in the body. As a result, toxicity due to overdose or ineffective treatment due to a lack of dose is difficult to avoid.¹¹ Therefore, the release of drugs from the MN system on demand is needed to balance the therapeutic effects and side effects. Several methods have been developed to provide on-demand drug release in MN by utilizing magnetic fields, ultrasound, and light.^{12–14} However, these methods were quite complicated and not safe for long-term use.

On-demand drug release can be done by using particular materials that have bioresponsive properties that can respond to physiological changes. The on-demand drug release system

using bioresponsive materials has been applied in the treatment of DM using glucose-responsive (GR) materials. In the presence of GR materials, drug release would occur in response to increased BGLs. As a result, drug release would increase with increasing BGLs and decrease when BGLs are normal.¹⁵ This system can prevent and reduce the risk of hypoglycemia from MTF. There are three types of GR materials that have been investigated for drug delivery for DM therapy, including phenylboronic acid (PBA) and its derivatives, con-canavalin A (Con A), and glucose oxidase (GOx). Con A and GOx are proteins that can be immunogenic, can be inactivated, less stable, and high cost. On the other hand, PBA is non-immunogenic, is more stable in vivo, and has a low cost.^{13,15,16} This study developed MTF delivery with a GR system using PBA attached to gelatin polymer. Gelatin is a natural polymer that has been widely used for drug delivery. Its structure consisting of amino and carboxyl groups gives it the advantage of undergoing structural modification with compounds from other materials.¹⁷

MTF will be encapsulated in PBA-attached gelatin. To prolong the release and permeation time, MTF will be formulated into microparticles (MPs). Many previous studies have shown that MPs can provide extended release.^{18,19} MTF and PBA MPs as a GR material (MP–MTF–GR) will be delivered transdermally through the dissolvable MN (DMN) system. DMN can penetrate the skin barrier, stratum corneum. When applied, the DMN polymer would form a number of pores as an aqueous channel that the drug would reach the deeper layers of the skin, without causing pain. Furthermore, the DMN polymer would directly enter the epidermis or upper dermis layer and go directly to the systemic circulation through a diffusion mechanism and show a therapeutic response when it reaches the site of action.^{20,21} In some studies, delivery via DMN is more practical because it could potentially deliver the drugs directly to the systemic circulation via dermis circulation more quickly than delivery via the oral route. This could increase bioavailability, provide sustained drug release, reduce unfavorable side effects, and improve pharmacological response.^{20,22} DMN consists of biocompatible and biodegradable polymers that can dissolve in the skin and leave no harmful sharp biohazards.²¹ Therefore, DMN that has been applied and removed from the skin can be disposed of without special treatment. Even in resource-poor settings, this DMN disposal can be done safely and securely. The polymers commonly used in DMN are water-soluble polymers, including polyvinyl pyrrolidone (PVP), polyvinyl alcohol (PVA), hyaluronic acid, maltose, dextran, albumin, and chondroitin sulfate.²³ Previous studies have shown that combining PVA and PVP as polymers in DMN provides adequate mechanical strength and penetration ability.²¹

In this study, for the first time, we developed a delivery system of MTF in the MP form incorporated in PBA-attached gelatin which was delivered transdermally through the DMN system with a combination of PVP and PVP polymers as a potential enhancer of T2DM therapy. The MP was characterized to select the optimum formulation which was further formulated into DMNs. Finally, MTF-loaded DMNs were evaluated for their release behavior in conditions mimicking hyperglycemic conditions in ex vivo studies. The outcomes of this study serve as a proof of concept for a new delivery system to selectively deliver MTF via the transdermal route to overcome the limitation of oral administration of MTF.

2. EXPERIMENTAL SECTION

2.1. Materials. MTF of analytical grade was purchased from Tokyo Chemical Industry Co., LTD, Tokyo, Japan. PBA, gelatin, acetic acid, glutaraldehyde, 1-ethyl-3(3-dimethylaminopropyl) carbodiimide hydrochloride (EDC·HCl), *N*-hydroxysuccinimide (NHS), dimethyl sulfoxide (DMSO), poly(vinyl pyrrolidone) [PVP (K30)], and poly(vinyl alcohol) PVA (10 kDa) were purchased from Sigma-Aldrich (Singapore). D-Glucose was obtained from Merck (Germany).

2.2. Preparation of Microparticle Metformin–Glucose Response. The MP–MTF–GR was prepared using a similar method from the previous study.¹⁷ Five formulations of MP–MTF–GR were prepared as shown in Table 1. Initially, the

Table 1. Composition of MP–MTF–GR

composition	(mg)				
	MP1	MP2	MP3	MP4	MP5
gelatin	100	150	200	250	300
MTF	100	100	100	100	100

predetermined amount of gelatin and 0.2 mL of acetic acid were added to 2 mL of water. To obtain a cloudy mixture, 5 mL of ethanol was added gradually. Then, as a cross-linking agent, 25 μ L of glutaraldehyde (25%) was added to the mixture. The mixture was then centrifuged at 7000 rpm for 15 min. The supernatant was taken out, and 3 mL of water was added to the precipitate (MP1). Subsequently, 12 mg of 3-CPBA was dissolved in 1 mL of DMSO. It was then reacted with 16.6 mg of EDC·HCl and 10 mg of NHS. The mixture was added to 3 mL of MP1 and stirred overnight at room temperature. To remove unreacted 3-CPBA, it was centrifuged at 7000 rpm for 1 min (MP2). Moreover, 100 mg of MTF was dissolved in MP2 and stirred overnight. To remove the unloaded MTF, the mixture was centrifuged at 9000 rpm for 15 min. Finally, MP–MTF–GR was obtained. The morphology of MP–MTF–GR was observed using a light microscope (Olympus CX23, Japan) and scanning electron microscope (FEI, Hillsboro, OR, USA).

2.3. Determination of Entrapment Efficiency and Drug Loading. The entrapment efficiency (EE) and drug loading (DL) were measured by centrifuging the formula for 15 min at 7000 rpm to separate the unencapsulated MTF. After that, the supernatant was taken; then, the absorbance was measured using a UV–visible spectrophotometer (Dynamica, HALO XB-10, Dynamica Scientific Ltd., Hong Kong) at a wavelength of 234.2 nm. The absorbance findings were then used to calculate the concentration of unencapsulated MTF, and then EE and DL were calculated using eqs 1 and 2 below.²⁴

$$\% \text{ EE} = \frac{(\text{wt of initial MTF} - \text{wt of unencapsulated MTF})}{\text{wt of initial mtf}} 100 \quad (1)$$

$$\% \text{ DL} = \frac{\text{amount of entrapped drug in microparticle}}{\text{total wt of microparticle}} 100 \quad (2)$$

2.4. Determination of Particle Size and Polydispersity Index. The particle size was determined by using the formula with a light microscope (Olympus CX23, Japan) with a magnification of 100 \times ; then, the particle size and polydispersity index (PDI) were measured using an Optilab Raster Image.²⁵

2.5. Determination of Zeta Potential. A total of 0.3 mg/mL of the formula was suspended in deionized water, and then the zeta potential was measured using a Mastersizer 2000 size analyzer (Malvern Instruments, Malvern, UK).¹³

2.6. Physicochemical Characterization of MP–MTF–GR Using Fourier Transform Infrared Spectroscopy. Initially, 2 mg of each sample was mixed with potassium bromide and compressed to form a pellet. Infrared (IR) spectra were recorded using a Fourier transform IR (FTIR) spectrometer (AccuTrac FT/IR-4100 Series, PerkinElmer, USA); spectra were collected in the wavelength range of 4000–400 cm^{-1} .¹³

2.7. Physical Form Characterization of MP–MTF–GR Using Differential Scanning Calorimetry and X-ray Diffraction. Physical characterization was carried out using differential scanning calorimetry (DSC) and X-ray diffraction (XRD) instruments. Analysis using DSC (DSC 2920, TA Instruments, Surrey, UK) was carried out by weighing as much as 3–5 mg by placing it on an aluminum pan and sealing it. The sample was then heated at a constant increase of 2 $^{\circ}\text{C}/\text{min}$ from 0 to 300 $^{\circ}\text{C}$ under a dry atmosphere of nitrogen.

Characterization using XRD was done by collecting XRD patterns using an XRD instrument (Rigaku Corporation, Kent, England) with Cu K α radiation. Then, the diffraction patterns were collected over the 2θ range of 0–50 $^{\circ}$.¹³

2.8. In Vitro Drug Release Study. The in vitro drug release study was carried out to observe the release of MTF from the MP–MTF–GR, MP–MTF, and pure MTF. This study was performed using the dialysis method. PBS and glucose-containing PBS (1, 2, and 4%) were used as the release medium. An amount of formulation (equivalent to 20 mg/mL of MTF) was inserted into the dialysis membrane. Then, it was placed in 100 mL of the release medium at 37 $^{\circ}\text{C}$. The release study was performed at 100 rpm. At predetermined time intervals (0.5, 1, 2, 3, 4, 5, 6, 7, 8, 12, and 24 h), an aliquot of 1 mL was taken and replaced by the same amount of fresh release medium. To determine the amount of drug released, samples were then analyzed using a UV–vis spectrophotometer (Dynamica, HALO XB-10, Dynamica Scientific Ltd., Hong Kong) at a wavelength of 234.2 nm. All measurement was done in triplicate. Furthermore, the data obtained were fitted to five different mathematical models using DD Solver software, namely, zero-order, first-order, Higuchi, Korsmeyer–Peppas, and Hixson–Crowell to determine the release kinetics of MTF.²⁶ The mathematical model is described in eqs 3–7

$$\text{Zero order: } C_t = C_0 + k_0 t \quad (3)$$

$$\text{First order: } \ln C_t = \ln C_0 + k_1 t \quad (4)$$

$$\text{Higuchi: } C_t = k_H \sqrt{t} \quad (5)$$

$$\text{Korsmeyer–Peppas: } C_t = k_{KP} t^n \quad (6)$$

$$\text{Hixson–Crowell: } C_t^{1/3} = C_0^{1/3} k_{HC} t \quad (7)$$

where C_t represents the percentage of MTF released at time t , C_0 represents the initial concentration of MTF in the medium, t represents the time, n represents the exponent of diffusion release, and k_0 , $k_1 k_{KP}$, k_H , and k_{HC} represent the release coefficient for zero order, first order, Korsmeyer–Peppas, Higuchi, and Hixson–Crowell, respectively.

To test the adaptability of GR–MP–MTF release depending on glucose levels in the medium, samples were first

incubated in a PBS medium containing 100 mg/dL glucose for 30 min. Afterward, the sample was removed and incubated in a medium containing glucose 400 mg/dL for 30 min.²⁷ This cycle was then repeated several times until 360 min. MTF released was then analyzed using a UV-vis spectrophotometer (Dynamica, HALO XB-10, Dynamica Scientific Ltd., Hong Kong) at a wavelength of 234.2 nm.

2.9. Formulation of Dissolving Microneedles Containing MP-MTF-GR. MP-MTF-GR-DMN was prepared using a silicone mold (needle density 20 × 20, pyramidal needles, 700 μm height). The aqueous blend of polymers containing various PVA and PVP concentrations was mixed with 25% w/w MP-MTF-GR. The concentration is presented in Table 2. Initially, 0.3–0.5 g of the mixture was

Table 2. Composition of MP-MTF-GR-DMN

formulation	composition (% w/w)			
	MP-MTF-GR	PVP	PVA	water
DMN1	25	25	10	40
DMN2	25	25	15	35
DMN3	25	25	20	30
DMN4	25	20	15	40
DMN5	25	15	15	45

poured into the silicone mold and then centrifuged at 3500 rpm for 30 min to fill the mold. DMN was then dried at room temperature for 24 h and dried at 37 °C for 24 h. The dried DMN was removed from the mold, and the morphology of the DMN was observed under a light microscope (Olympus CX23, Japan).

2.10. Evaluation of Mechanical Strength and Penetration Properties of MP-MTF-GR-DMN. The mechanical strength of DMN was evaluated using a TA.TX2 texture analyzer in compression mode as in the previous study.²¹ DMN was given a force of 32 N/array for 30 s. DMN was observed using a light microscope (Olympus CX23, Japan), and the height before and after the test was determined using Image Raster software. The percentage reduction in needle height was calculated by eq 8, where h_B is the height before testing and h_A is the height after testing.

$$\% \text{ Height needle reduction} = \frac{h_B - h_A}{h_B} \times 100 \quad (8)$$

Penetration properties of DMN were evaluated using ParafilmM as a validated artificial skin model.²⁸ DMN was applied to eight layers of ParafilmM and given a force of 32 N/array for 30 s. The number of holes formed in each layer was calculated, and the deepest layer of the hole was determined.

2.11. Calculation of Theoretical Drug Content in Needles and Determination of Drug Recovery. Theoretical drug content was determined by calculating the densities of all formulas first. To calculate the density of the formula, the blank polymer mixture (without MP-MTF-GR) was prepared on a flat block and then dried. The dried blocks were weighed, and the dimensions were measured to determine the volume. The volume of the block was calculated by eq 9.

$$\text{Volume} = \text{width} \times \text{length} \times \text{height} \quad (9)$$

The density of formulas was determined by eq 10.

$$\text{Density} = \frac{\text{mass}}{\text{volume}} \quad (10)$$

The needle volume was determined using the dimensions of the needle, and then the mass of the needle was determined using the volume of needles and density of formulas. The mass of MP in the needle was determined by calculating the percentage of dry MP in needle mass. Finally, the MTF content theoretically was calculated by eq 11.

$$\text{MTF content in needle} = \text{drug loading} \times \text{mass of MP in needle} \quad (11)$$

The drug content was determined by dissolving DMN in 5 mL of distilled water. 10 mL of methanol was added to this mixture, and then the mixture was sonicated for 30 min. Then, this mixture was centrifuged at 5000 rpm for 10 min and the supernatant was collected. The absorbance of MTF was determined using a UV-vis spectrophotometer (Dynamica, HALO XB-10, Dynamica Scientific Ltd., Hongkong) at a wavelength of 234.2 nm, and the concentration was determined (concentration found). Drug content recovery was determined using eq 12.

$$\text{Drug content recovery (\%)} = \frac{\text{concentration found}}{\text{theoretical drug content}} \times 100 \quad (12)$$

2.12. Evaluation of Surface pH. In this study, 20 mg of MNs were stored in a beaker containing 50 mL of double-distilled water, and then the MNs were allowed to swell for 15 min at room temperature. To measure the pH value, a pH meter (Horiba Scientific, Kyoto, Japan) was used. A composite glass electrode was held close to the surface of the MN to be measured. The pH was then measured after an equilibration time of 1 min.²⁹

2.13. Evaluation of the Water Vapor Transmission Rate. The water vapor transmission rate (WVTR) was assessed using a glass vial containing 1 g of anhydrous calcium chloride. DMN was sealed in a glass vial with the help of adhesive tape. This vial was then placed in a desiccator containing a saturated solution of potassium chloride (% RH 85%). The vial was weighed at a predetermined time. The WVTR was calculated by eq 13

$$\text{WVTR} = \frac{(\text{final mass} - \text{initial mass of vial}) \times \text{thickness of DMN}}{\text{surface area}} \quad (13)$$

2.14. Evaluation of Moisture Absorption Ability. Moisture absorption ability (MAA) testing was carried out using the method from the previous study.³⁰ MAA testing was conducted to determine the ability of DMN to absorb moisture at different % RH. DMN was placed in different desiccators. The desiccator contained magnesium chloride (33% RH), sodium nitrite (69% RH), and potassium sulfate (97% RH). MN weights were measured every 48 h for 14 days. % MAA was calculated by eq 14.

$$\% \text{ MAA} = \frac{\text{final mass} - \text{initial mass}}{\text{initial mass}} \times 100 \quad (14)$$

2.15. Dissolution Study. A dissolution time test was carried out using rat skin to determine the time required for DMN to dissolve in the skin completely. Rat skins were obtained from sacrificed rats. All animal studies were approved

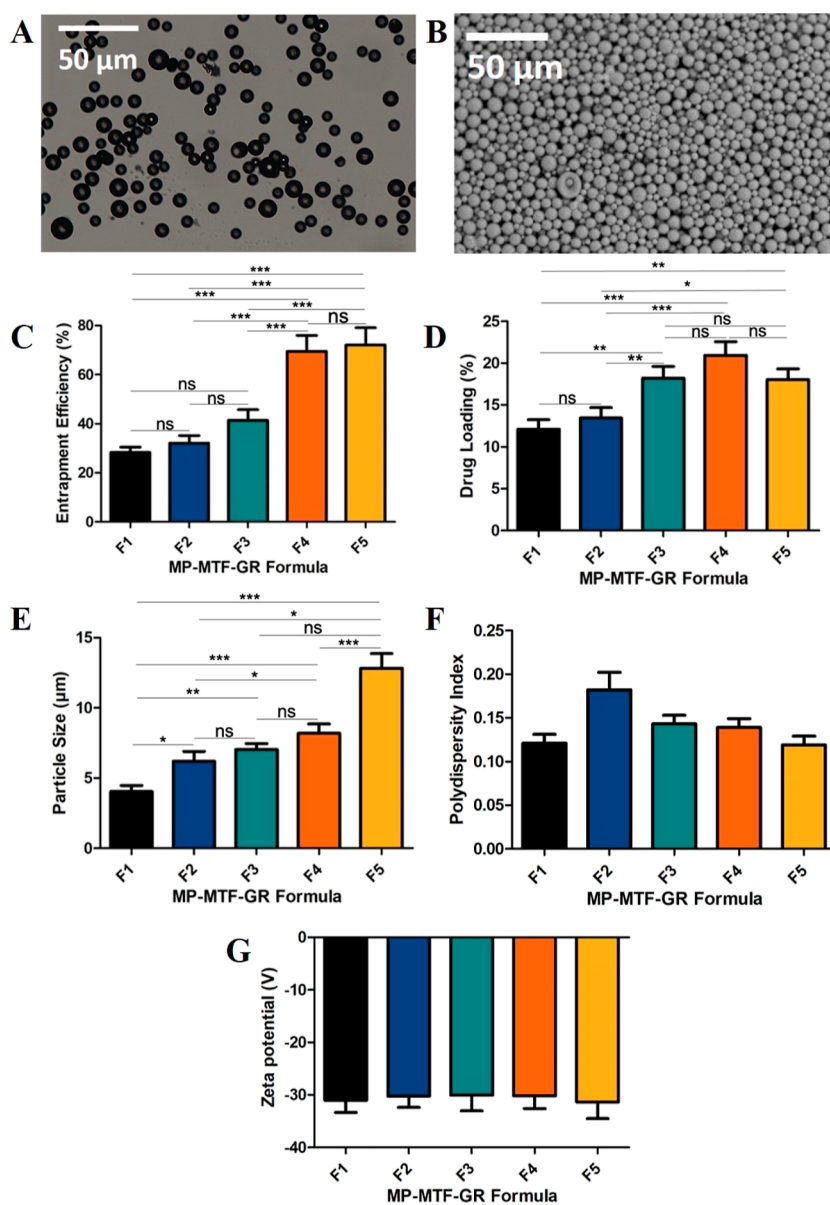


Figure 1. (A) Microscopic image, (B) SEM images, (C) EE, (D) DL, (E) particle size, (F) PDI, and (G) zeta potential of MP–MTF–GR (means \pm SD, $n = 3$).

by the Ethics Committee of the Faculty of Medicine, Hasanuddin University (protocol number: UH22070351). Rat skin was carefully shaved using a spatula and hair removal cream. The skin was excised at full thickness and then soaked and cleaned with saline solution to remove the fat on the skin.

DMN was applied to the rat skin, and manual pressure was applied to ensure penetration. Above the DMN was placed a 5 g stainless-steel cylinder (11 cm) to ensure that the DMN does not move from its place. At a predetermined time, DMN was removed and DMN morphology was observed under a light microscope (Olympus CX23, Japan). The dissolution test was carried out until the DMN was completely dissolved.

2.16. Ex Vivo Permeation Study. An ex vivo permeation study was carried out to obtain MTF permeation profiles of DMN containing MP–MTF–GR, MP–MTF, and pure MTF on media PBS pH 7.4 and glucose-containing PBS (1, 2, and 4%). This study was performed using Franz diffusion cells. Rat skin was used as a permeation membrane and placed between the donor compartment and receptor compartment in Franz

cells with the stratum corneum facing upward. DMN was applied in the center of the skin by using manual pressure for 30 s. A 5.0 g cylinder was placed over the DMN to ensure that DMN stayed in its place. In the receptor compartment, PBS pH 7.4 medium was placed using a normal body fluid model, and PBS + glucose 1%, PBS + glucose 2%, and PBS + glucose 4% were used as the body fluid models with increased glucose levels. The medium was stirred at 100 rpm, and the temperature was maintained at 37 ± 1 °C. The donor compartment was placed above the receptor compartment and was sealed using ParafilmM to reduce evaporation. 0.5 mL of medium was sampled through the sampling arm and replaced by the same amount of fresh medium at predetermined time intervals (0.25, 0.5, 0.75, 1, 2, 3, 4, 5, 6, 7, 8, and 24 h). The absorbance of sampled media was determined using a UV–vis spectrophotometer (Dynamica, HALO XB-10, Dynamica Scientific Ltd., Hong Kong) at a wavelength of 234.2 nm. The concentration obtained was plotted against the sampling time.

2.17. In Vivo Study in Diabetic Rats. The Ethics Committee of Medical Faculty Hasanuddin University approved the animal research protocol. In this study, 30 male Wistar rats were used, weighing 220.36 ± 9.62 g.

Wistar rats were induced with T2DM using streptozotocin (STZ). Induction of T2DM was carried out in the diabetes group ($n = 25$) using two low-dose injections of STZ (100 mg/kg) in 0.1 M citrate buffer (pH 4.5) by intraperitoneal injection. FBG levels were measured after 8 days of STZ injection using a glucose meter (Nesco Multicheck). Rats with FBG levels of more than 400 mg/dL were considered diabetic and used in further analysis.

Rats were grouped into six groups ($n = 5$): healthy group, control group, oral group, DMN group, DMN without PBA group, and pure MTF–DMN group. Groups of healthy rats were prepared by providing a standard feed without diabetes induction. The control group was prepared by inducing T2DM using STZ and maintaining BGLs. The oral group was prepared by giving MTF tablets with a dose of 100 mg/kg body weight to rats induced by T2DM. All rats in the DMN, DMN without PBA, and pure MTF–DMN groups were treated transdermally with DMN (DMN with GR compound), DMN without PBA (DMN without GR compound), and pure MTF–DMN (DMN without MP) as much as six patches which were equivalent to the dose of $75.58 \mu\text{g}/\text{patch}$ ($453.48 \mu\text{g}$ in total). Rat blood was collected from veins in the tail at intervals of 0, 1, 2, 3, 4, 5, 6, 7, 8, 9, 10, and 12 h to detect BGLs using a glucose meter (Nesco Multicheck). Additionally, to evaluate the skin integrity, before and after the experiment, the skin moisture of the rats was analyzed using a skin moisture analyzer (Skin Analyzer VCare Mode SK-8, Vcare, India).

2.18. Hemolysis Test. The hemolysis test was carried out using the erythrocytes from rats by centrifuging whole blood for 20 min at 2000 rpm. The collected erythrocytes were then washed using PBS with three washing cycles. After that, the erythrocytes were resuspended in PBS to obtain a concentration of 10% v/v. After that, the suspension was added to the sample with a concentration of 500, 50, and 5 g/mL.

Next, the mixture was incubated at 37°C for 1 h, followed by centrifugation at 7000 rpm for 10 min. Finally, the absorbance of the supernatant from the centrifugation was measured using a UV–vis spectrophotometer (Dynamica, HALO XB-10, Dynamica Scientific Ltd., Hong Kong) at 540 nm to estimate the number of free erythrocytes. PBS and distilled water were used as positive and negative controls, respectively.²⁹

The percentage of hemolysis was calculated using eq 15

$$\text{Hemolysis (\%)} = \frac{\text{abs (test sample)} - \text{abs (negative control)}}{\text{abs (positive control)} - \text{abs (negative control)}} \times 100 \quad (15)$$

where “abs” is the absorbance.

2.19. Statistical Analysis. All data are shown as mean \pm standard deviation (SD) of the mean. All values were obtained using Microsoft Excel (Microsoft Corporation, Redmond, USA). GraphPad Prism version 5.03 (GraphPad Software, San Diego, California, USA) was used for statistical analysis. One-way ANOVA was used to analyze multiple groups, while the *t*-test was used to analyze two groups. In all cases, $p < 0.05$ was considered as a significant difference.

3. RESULTS AND DISCUSSION

3.1. Preparation of Microparticle Metformin–Glucose Response. In this study, MTF was formulated into glucose-sensitive MP. MP delivery systems offer various advantages, including adequate protection and prolonged effects of drugs.¹⁹ Gelatin and PBA were used as the polymer and glucose-sensitive agents, respectively. The MP fabrication was carried out by cross-linking gelatin with glutaraldehyde through the nucleophilic addition-type reaction between the aldehyde groups with free nonprotonated ϵ -amino groups of lysine or hydroxylysine.³¹ Furthermore, PBA was loaded into the MP to obtain the glucose-sensitive release of MTF to avoid its adverse effect. The morphology of MP–MTF–GR was observed using a light microscope and SEM, as presented in Figure 1A,B, showing that the formulation possessed a shape form. All formulations were evaluated to obtain the optimum formulation.

3.2. Determination of EE and DL. EE is an important parameter that informs the percentage of drugs successfully entrapped into the MPs.³² In the MP–MTF–GR system, the MTF was entrapped in the polymer matrix due to cross-linking between gelatin and glutaraldehyde. The value of EE obtained is shown in Figure 1C. It could be observed that higher polymer concentration would result in a higher EE value due to the prevention of drug diffusion across continuous phases.³³ Analyzed statistically, the EE value for MP1, MP2, and MP3 was significantly different ($p > 0.05$). Furthermore, it was found that the EE value of MP4 ($69.53 \pm 6.46\%$) was significantly higher than MP3 ($p < 0.05$) but exhibited nonsignificant differences from the EE value of MP5 ($p > 0.05$). Therefore, in order to minimize the use of an excipient in the formulation, MP4 was chosen as the optimum formulation and was further investigated.

DL measurement is one of the key parameters. It was performed to determine the amount of the total entrapped drug compared to the total MP weight. The DL value obtained is shown in Figure 1D. Subsequently, the DL value for MP1, MP2, MP3, MP4, and MP5 was 12.09 ± 1.15 , 13.43 ± 1.24 , 18.21 ± 1.38 , 20.93 ± 1.63 , and $18.02 \pm 1.28\%$, respectively. All formulations showed a high DL value, which is $>10\%$.³⁴

3.3. Determination of Particle Size and PDI. The result of the particle size analysis was shown in Figure 1E. Subsequently, the particle size was found to be 4.04 ± 0.43 , 6.19 ± 0.71 , 7.03 ± 0.43 , 8.19 ± 0.66 , and $12.83 \pm 1.04 \mu\text{m}$ for MP1, MP2, MP3, MP4, and MP5, respectively. The particle size of all formulations was significantly different ($p > 0.05$). It could be observed that there is an increase in particle size with higher polymer concentration, probably due to the tendency of the polymer to coalesce.

In order to determine the heterogeneity of the MPs based on the size, PDI measurement was carried out. The result obtained is shown in Figure 1F. The PDI value ranged from 0 to 1. A low PDI value indicates a perfectly uniform sample with respect to particle size, while a high PDI value indicates highly polydisperse particles. A PDI value <0.2 is considered acceptable for polymer-based systems.²⁵ Therefore, it can be concluded that all formulations showed the desired PDI value, which is < 0.2 . This finding implies that the formulation is monodisperse.

3.4. Determination of Zeta Potential. The zeta potential is one of the parameters that can be used to ensure the stability of MPs developed from a physical point of view.¹³ The results

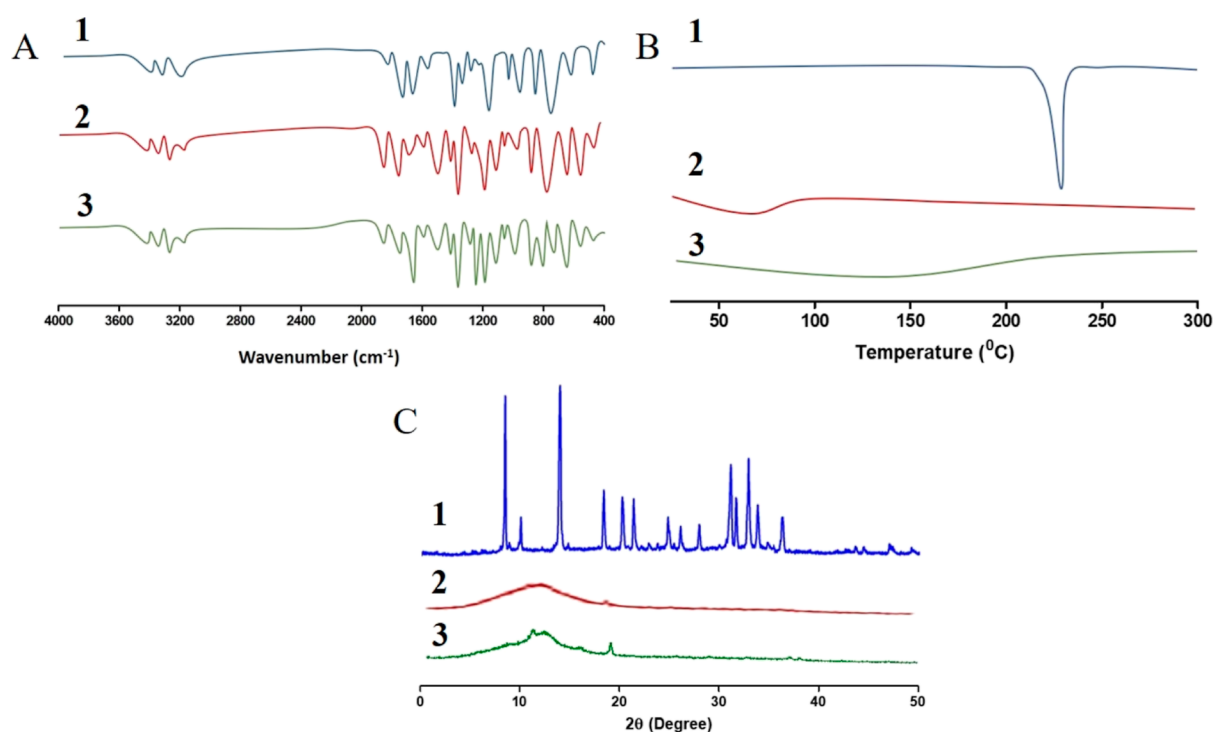


Figure 2. (A) FTIR spectra, (B) DSC thermogram, and (C) X-ray diffractogram of (1) pure MTF, (2) MP-MTF, and (3) MP-MTF-GR.

of the zeta potential measurements of all formulas are shown in Figure 1G. It is found that all formulas have high zeta potential values, which are above -30 mV. This value indicates a stable suspension particle shape and is not susceptible to rapid coagulation or flocculation.¹⁹ The PBA matrix linked to the gelatin polymer in incorporating MTF has many hydroxyl groups from PBA as well as carbonyl groups from gelatin which gives a negative charge on the surface of the MPs. This explains the negative charge obtained in the zeta potential measurement results from all formulas.¹⁷

3.5. Physiochemical Characterization of MP-MTF-GR Using Fourier Transform Infrared Spectroscopy. The presence of MTF in the developed MP system can be determined by characterization using FTIR spectroscopy. The results of the characterization of pure MTF using FTIR spectroscopy can be seen in Figure 2A, showing peaks at 3369 and 3295 cm^{-1} and indicating the presence of NH-stretching, which is a typical group possessed by the MTF structure.³⁵ In addition, CN-stretching was seen at 1619 and 1568 cm^{-1} , CH-stretching was seen at 3181 , and CH deformed at 929 cm^{-1} . It can be seen that the IR MP spectrum containing MTF shows the same peaks as in the pure MTF IR spectrum. This indicates that the MTF in the MP formula does not undergo structural changes and indicates the presence of MTF trapped in the MP system. In addition, the formula containing PBA (F4) showed a peak at 1639 cm^{-1} , which indicated the C=O amide stretching vibration of PBA and a peak at 1319 cm^{-1} due to bending vibrations from benzene and stretching vibrations from boric acid, which indicates that PBA was successfully attached to the MP.

3.6. Physical Form Characterization of MP-MTF-GR Using DSC and XRD. The presence and physical form of MTF in MPs can be determined by characterization using DSC and XRD spectroscopy. The results of physical characterization using DSC are shown in Figure 2B. The endothermic relaxation of pure MTF was seen at a sharp peak

formed at 234 °C, indicating pure MTF in crystalline form; this shows similarities to the previous research literature.³⁶ This sharp peak then disappeared, and amorphous endothermic relaxation was observed in the MP DSC data, both with PBA (F4) and MP without PBA (F4 without PBA). These findings indicate that the MTF formulated as MP is perfectly encapsulated in the polymer matrix. These findings were supported by the XRD characterization results shown in Figure 2C. The XRD pattern of pure MTF shows a sharp peak at 2θ of 10 – 50° which indicates the crystalline form of MTF. Similar to the DSC data findings, the F4 formula without PBA produces an XRD pattern with wide and sloping peaks. This shows the amorphous diffraction pattern in formula F4 without PBA. In addition, the semicrystalline structure of formula F4 is characterized by XRD patterns with wide peaks. However, at $2\theta = 19^\circ$, sharp peaks were seen, probably coming from the crystalline form of PBA linked by gelatin.³⁷

3.7. In Vitro Drug Release Study. The in vitro release behavior of pure MTF, MP-MTF (F4 without PBA), and MP-MTF-GR (F4) in four different release media is illustrated in Figure 3. The result clearly showed that after 2 h, pure MTF was completely released in all media. Specifically, MFT release from pure MTF was 98.12 ± 9.11 , 99.01 ± 8.31 , 97.05 ± 9.21 , and $98.0 \pm 9.19\%$ in PBS, glucose-containing PBS (1%), glucose-containing PBS (2%), and glucose-containing PBS (4%), respectively. The analysis statistically showed that no significant difference was found in the release of MTF from pure MTF in all media ($p > 0.05$). This result implies that the release of MTF from pure MTF is not affected by the presence of glucose.

For MP-MTF, after 24 h, the release of MTF in PBS, glucose-containing PBS (1%), glucose-containing PBS (2%), and glucose-containing PBS (4%) was 97.01 ± 8.13 , 96.93 ± 8.83 , 98.09 ± 9.3 , and $99.19 \pm 9.16\%$, respectively. Despite the difference, the MTF release profile from F4 without PBA was not significantly different ($p > 0.05$). Similar to the released

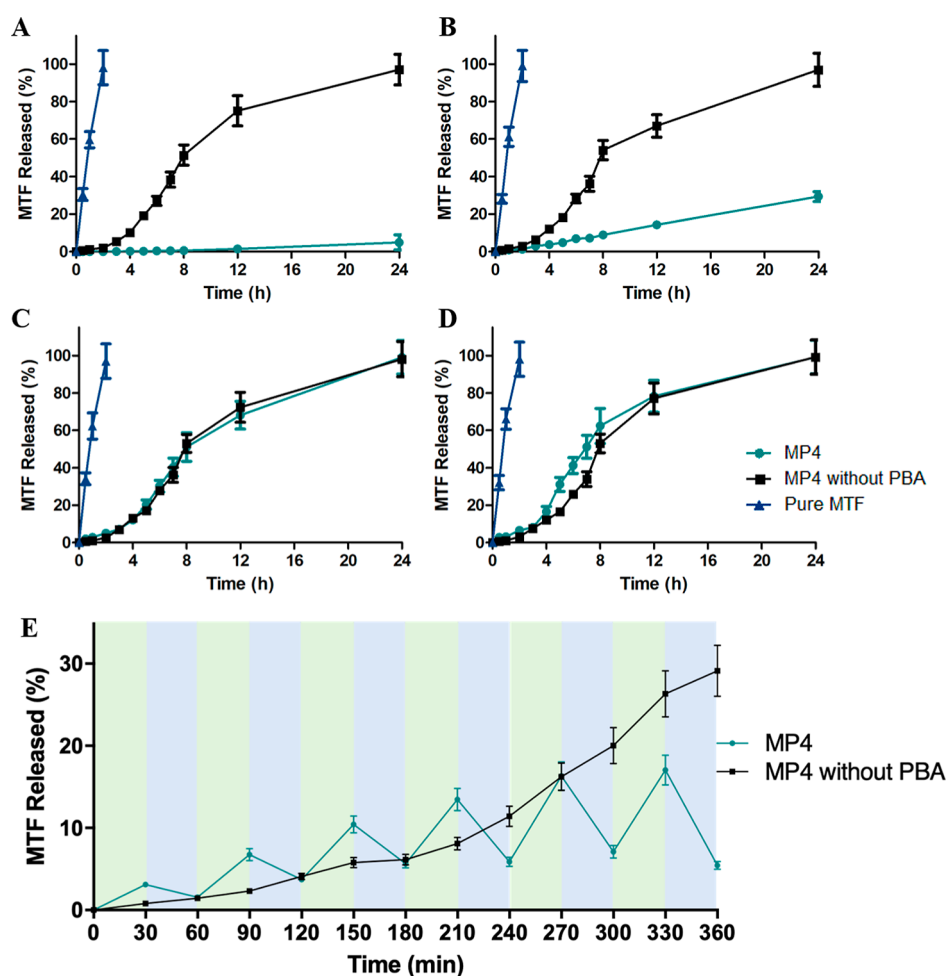


Figure 3. In vitro drug release of MP4, MP4 without PBA, and pure MTF in (A) PBS medium, (B) PBS + glucose 1% medium, (C) PBS + glucose 2% medium, and (D) PBS + glucose 4% medium. (E) Pulsatile release profile of MP4 and MP4 without PBA in media with glucose concentrations of 100 (blue) and 400 mg/dL (green) (means \pm SD, $n = 3$).

profile from pure MTF, formulation of MTF in the form of MP–MTF exhibited release behavior that did not depend on the absence/presence of glucose. Compared to the release profile from pure MTF, it was observed that the formulation of MTF into MPs could prolong the release of MTF up to 24 h by following previous studies.^{18,19} This was due to the cross-linking of gelatin in the MP formulation.³⁸ These findings indicated that the formulation of MTF into MPs was crucial to obtaining prolonged drug release.

Conversely, the release profile of MTF from MP–MTF–GR was found to decrease significantly in PBS compared to pure MTF and MP–MTF ($p < 0.05$). After 24 h, only $4.98 \pm 3.98\%$ of MTF was released. As the concentration of glucose in the medium increased, a higher amount of MTF was released from MP–MTF–GR. Subsequently, 29.34 ± 2.64 , 99.09 ± 8.92 , and $99.18 \pm 8.93\%$ of MTF were released after 24 h in glucose-containing PBS (1%), glucose-containing PBS (2%), and glucose-containing PBS (4%), respectively. This indicates successful GR drug delivery of MTF. The GR effect was obtained by the addition of PBA into the formulation as a glucose-sensitive agent. PBA exhibited a reversible reaction with the *cis*-diol compound, found in the glucose structure, through boronate formation. There are two forms of PBA in an aqueous solution, the hydrophobic neutral trigonal-planar and the hydrophilic negatively charged tetrahedral boronate. There

is an equilibrium between these two forms. Both forms bind specifically to 1,2- or 1,3-diols found in glucose to form a cyclic boronic ester. This binding leads to increased hydrophilicity of PBA-containing materials, thus inducing swelling and disassembling of the drug carrier, resulting in glucose-triggered drug release.³⁹

To determine the release kinetics of MTF from GR–MP–MTF, the in vitro release data were fitted to several mathematical models. The results showed that MTF exhibited Korsmeyer–Peppas kinetics following testing in PBS, glucose-containing PBS (1%), and glucose-containing PBS (2%) with a correlation coefficient of 0.9993, 0.9980, and 0.9403, respectively. In glucose-containing PBS (4%), MTF showed Hixson–Crowell kinetics with a correlation coefficient of 0.9358. The Korsmeyer–Peppas kinetics describe drug release from polymeric systems. Moreover, the Hixson–Crowell kinetics describes release from systems with a change in surface area and diameter of particles.⁴⁰

Figure 3E shows a pulsating profile of MTF release from the MP–MTF–GR formula in each incubation medium. It was found that less MTF was released when the formula was incubated in a medium containing glucose 100 mg/dL, and a high drug release was achieved when the formula was incubated in a medium containing glucose 400 mg/dL. A significant difference ($p < 0.05$) was obtained in the MP–MTF

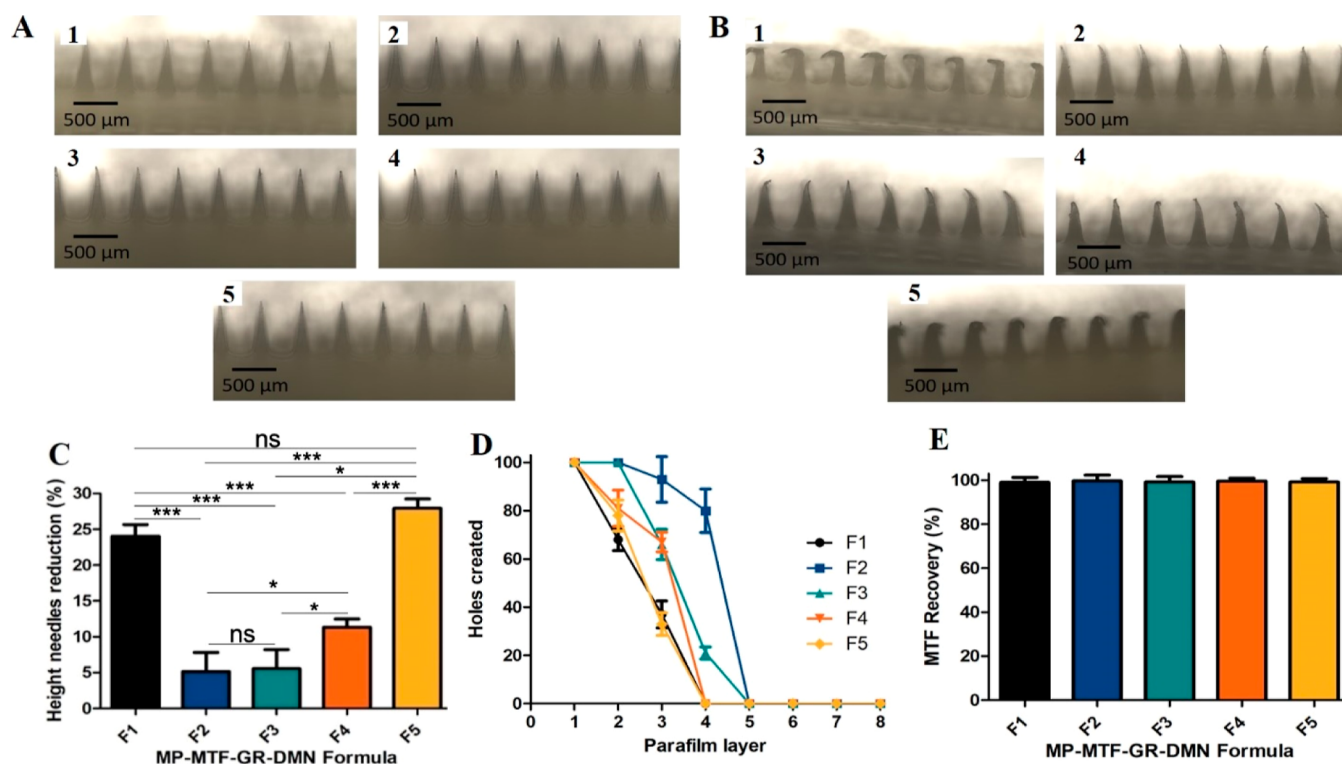


Figure 4. Microscopic image of MP-MTF GR dissolvable MN (A) before evaluation and (B) after evaluation of DMN1 (1), DMN2 (2), DMN3 (3), DMN4 (4), and DMN5 (5). (C) Mechanical strength, (D) penetration properties, and (E) MTF recovery of MP-MTF GR dissolvable MN (means \pm SD, $n = 3$).

formula without the GR compound. A constant and unchanged release profile was obtained during the change of the incubation medium. This shows that the release of MTF from the MP-MTF-GR formula could adapt according to changes in BGLs in the medium.

3.8. Formulation of DMN Containing MP-MTF-GR.

In this study, an aqueous blend of PVA and PVP was used in the DMN formulation with various concentrations, as shown in Table 2. Previous studies have shown that the combination of these two polymers results in better mechanical strength and penetration ability than when used singly.^{21,23} PVP is a polymer with good hardness, but when used alone, it will provide inadequate mechanical strength for DMN due to its hygroscopicity.^{23,41} The addition of PVA will fix the shortcomings of PVP. The combination of PVA and PVP causes the formation of hydrogen bonds between the C=O group of PVP and the -OH group of PVA to provide adequate mechanical strength.²⁶ All formulas were added with MP-MTF-GR with the same concentration, 25% w/w. The MP-MTF-GR concentration in DMN is the optimal concentration of drug particles and does not affect the physical characteristics of the DMN. This concentration is not a regular concentration that can provide pharmacological effects by transdermal delivery. This is because this study only aims to prove the concept, and further research is needed to discuss pharmacokinetic tests to determine the bioavailability of MTF and the concentration of MTF that is capable of providing pharmacological effects from this transdermal delivery. Figure 4A shows the morphology of all DMN containing MP-MTF-GR obtained using a light microscope. All formulations resulted in a homogeneous polymer blend with the DMN that formed a sharp needle tip.

3.9. Evaluation of Mechanical Strength and Penetration Properties of MP-MTF-GR-DMN.

The mechanical strength of the DMN was evaluated to assess the ability of the DMN to withstand compression. The resistance of the DMN to compression is important because the DMN must be applied by manual compression to ensure that the DMN penetrates the stratum corneum. Furthermore, the mechanical strength was evaluated by providing a force of 32 N/array equivalent to manual compression strength. The morphology of MP-MTF-GR-DMN after the evaluation was obtained using a microscope and is shown in Figure 4B. The percentage reduction in needle height after compression indicates the mechanical strength of DMN.²⁶ The results of this evaluation are shown in Figure 4C. The percentage reduction in needle height was 24.02 ± 1.63 , 5.14 ± 2.66 , 5.55 ± 2.67 , 11.32 ± 1.17 , and $27.92 \pm 1.30\%$ for DMN1, DMN2, DMN3, DMN4, and DMN5, respectively. Interestingly, the percentage of needle height reduction in DMN2 and DMN3 was $<10\%$ and significantly different ($p < 0.05$) compared to that of all formulas, which resulted in adequate mechanical strength.

Penetration ability was evaluated by using eight layers of ParafilmM. These parafilm layers were developed as an artificial skin model and validated in previous studies.²⁸ The results of the evaluation of the penetration ability (Figure 4D) showed that DMN1, DMN4, and DMN5 penetrated only until the third layer of parafilm equivalent to $378 \mu\text{m}$ of the total needle height of $700 \mu\text{m}$ or 54% of the total needle height. On the other hand, DMN2 and DMN3 could penetrate deeper up to the fourth layer of parafilm equivalent to a thickness of $504 \mu\text{m}$, indicating that 72% of the needles could penetrate. Furthermore, there was no significant difference ($p > 0.05$) between the number of holes formed in the fourth layer compared to DMN2 and DMN3. However, the number of

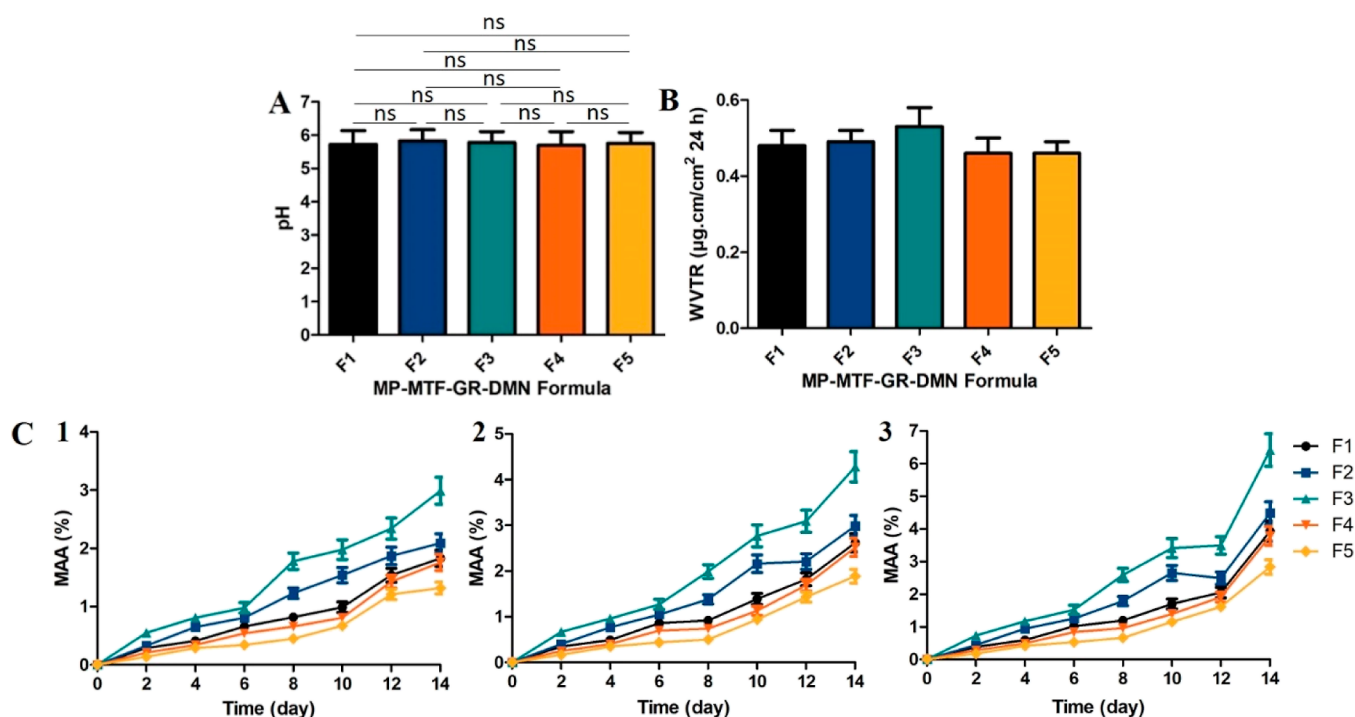


Figure 5. Evaluation of the (A) pH surface and (B) WVTR of MP–MTF GR dissolvable MN. (C) MAA of MP–MTF GR dissolvable MN in (1) RH 33%, (2) RH 69%, and (3) RH 97% (means \pm SD, $n = 3$).

holes formed by DMN2 was more than that by DMN3, indicating better penetration ability. Based on the result, DMN2 was considered for further tests.

In applying the MNs, an applicator can ensure that the pressure applied to the MN is appropriate so that the needle can be inserted entirely into the stratum corneum. An example of a commonly used applicator is a spring-operated applicator specially designed for MN insertion.⁴² In addition, a previous study has provided an innovation in applying MNs to the stratum corneum by using a pressure-indicating sensor film that would change color when the applied force reaches 30 N, and the color would be more concentrated when a greater force is applied. Based on previous research, the minimum pressure required to insert a MN array of 1 cm² into the stratum corneum is 32 N cm⁻².⁴³

3.10. Calculation of Theoretical Drug Content in Needles and Determination of Drug Recovery. Before determining the drug content in the needle, it is necessary to determine the density of the DMN formula. The DMN density was found to be 1.05 ± 0.01 , 1.06 ± 0.01 , 1.06 ± 0.06 , 1.07 ± 0.02 , and 1.07 ± 0.01 mg/mm³ for DMN1, DMN2, DMN3, DMN4, and DMN5, respectively. Theoretically, the weights of MTF in needles were found to be 81.44, 75.58, 71.43, 82.64, and 91.08 g for DMN1, DMN2, DMN3, DMN4, and DMN5, respectively. Furthermore, the MTF content in the formula was determined using a UV–vis spectrophotometer and compared with the theoretical weights. The drug recovery for all formulas is shown in Figure 4E. Drug recovery obtained is in the range of drug recovery requirements by ICH, 95–105%.⁴⁴ This indicates that the formulation of MTF in the form of MPs with additional glucose response reformulated in DMN did not affect the concentration of MTF.

3.11. Evaluation of Surface pH. One of the important things to consider in the formulation of intradermal dosage forms is the surface pH. This is important to note because

human skin can undergo reactions that can create discomfort when in contact with materials with a pH that is incompatible with the pH that can be tolerated by human skin. The results of the surface pH evaluation of the MP–MTF–GR–DMN formula can be seen in Figure 5A. From the evaluation results, the MP–MTF–GR–DMN formulas DMN1, DMN2, DMN3, DMN4, and DMN5 had surface pH values of 5.72 ± 0.34 , 5.78 ± 0.32 , 5.69 ± 0.41 , and 5.75 ± 0.33 , respectively. The surface pH value of each formula was not significantly different ($p > 0.05$) and showed a safe pH value for the skin, which was 4.1–5.8.⁴⁵ This indicates that the MP–MTF–GR–DMN formula is safe to apply to human skin without causing irritation or other things that can cause discomfort.

3.12. Evaluation of WVTR. Evaluation of the WVTR was carried out to assess the integrity of DMN against high humidity in storage. The WVTRs of all formulas are shown in Figure 5B. The WVTR increases with increasing polymer concentration. This is because the WVTR increases with increasing polymer hydrophilicity.⁴⁶ However, this increase was not statistically significant ($p > 0.05$). After 7 days, the WVTR of all formulas obtained was lower than that of the previous study.⁴⁷ A low WVTR indicates the ability of the DMN to maintain its integrity against high humidity and exhibits the long-term stability of the DMN.

It is important to remember that the WVTR does not affect DMN dissolution when applied to the skin. The selection of biodegradable polymers and the presence of interstitial fluid and skin elasticity can cause damage to the integrity of DMN and quickly dissolve after insertion.⁴⁸

3.13. Evaluation of MAA. MAA is one of the crucial tests of DMN. The ability to absorb moisture from the outside during the storage period can affect the mechanical strength and penetration ability of DMN. In this study, we used three levels of humidity. The results can be seen in Figure 5C. After 14 days, the moisture absorption of all formulas at all humidity

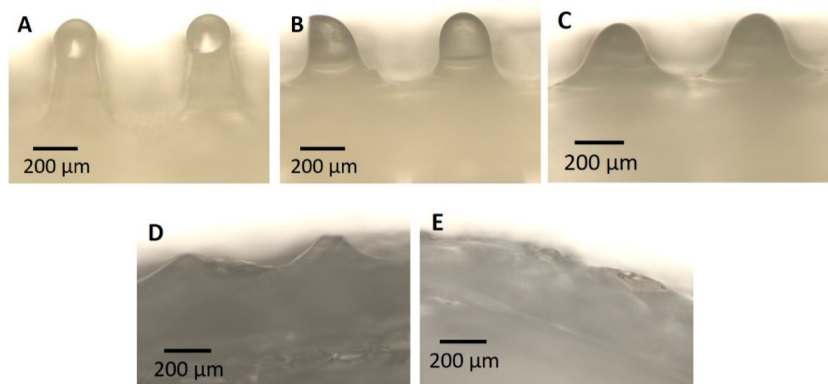


Figure 6. Microscopic image of the dissolution of DMN2 at (A) 3, (B) 6, (C) 9, (D) 12, and (E) 15 min.

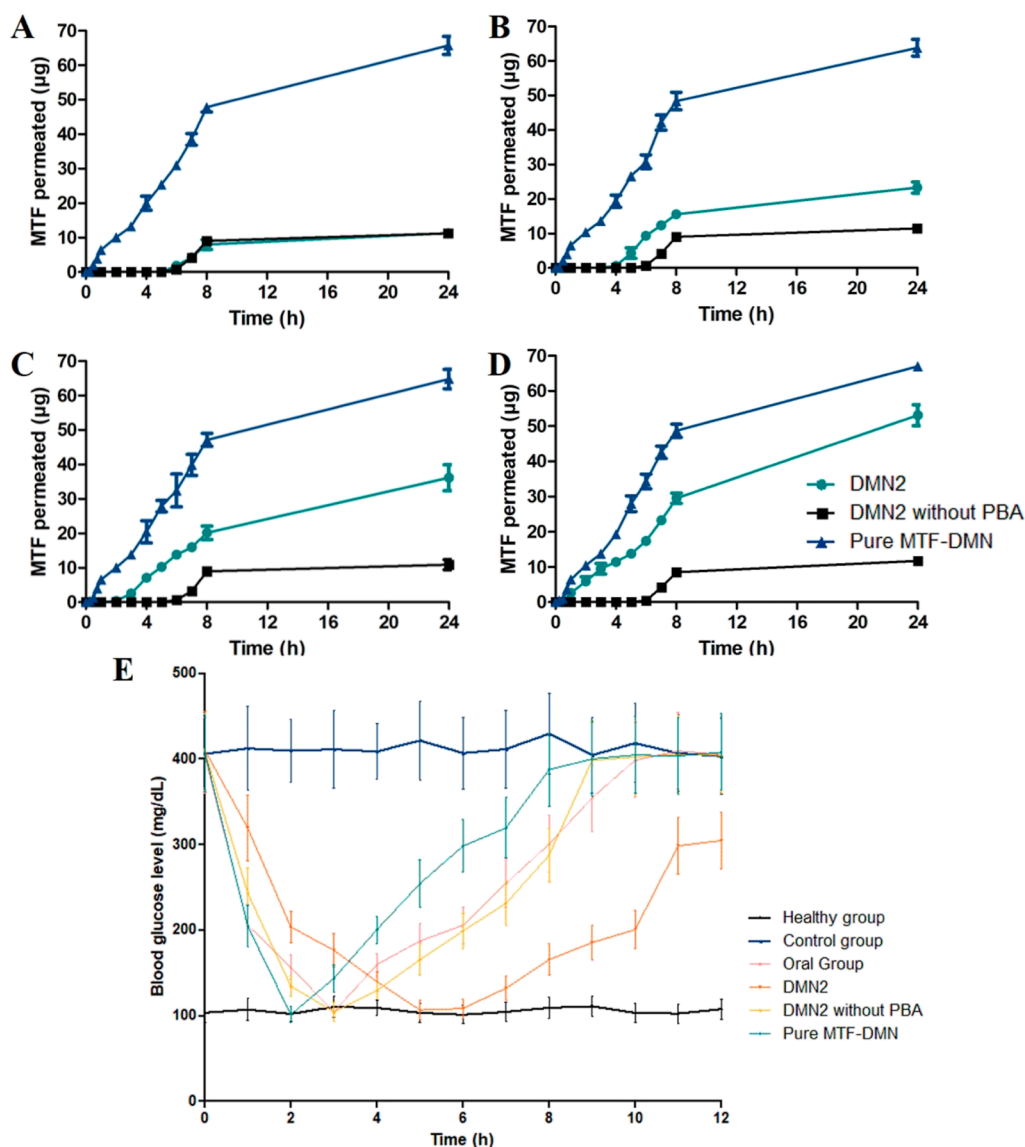


Figure 7. Ex vivo permeation of DMN2 (MP–MTF GR dissolvable MN), DMN2 without PBA (MP–MTF-dissolvable MN), and pure MTF-dissolvable MN in (A) PBS media, (B) PBS + glucose 1% media, (C) PBS + glucose 2% media, and (D) PBS + glucose 4% media (means \pm SD, $n = 3$). (E) BGLs of the diabetic rat model following the administration of DMN, DMN without PBA, and pure MTF–DMN and MTF orally (means \pm SD, $n = 5$).

was found to be below 10%. In all formulas, moisture absorption increases with increasing humidity. The MAA of

each formula was also different. The MAA increases as the concentration of polymer in the formula increases. The highest

MAA was obtained at DMN3, followed by DMN2, DMN1, DMN4, and DMN5. The increase in MAA according to the polymer concentration was due to the hygroscopicity of the polymers used in both PVP and PVA. PVP and PVA are hygroscopic polymers because their structure contains hydrophilic groups, namely, carbonyl and hydroxyl groups.^{30,41} The carbonyl and hydroxyl groups can bind with water in the environment to form hydrogen bonds.

3.14. Dissolution Study. Dissolution time is an important test of DMN. According to its characteristics, DMN must be soluble when applied to the skin. The dissolving time test results are given in Figure 6. DMN2 was found to dissolve completely within 15 min, with a decrease in needle height after 3 min of observation. DMN application duration can be determined from the DMN dissolving time; it is obtained that for effective delivery, needles containing drug MPs must completely dissolve in the skin. Based on the dissolution time test, the time required for DMNs to dissolve entirely in the skin is 15 min. Therefore, for full drug delivery, it is recommended to apply the DMN to the skin for 15 min, and then it can be removed from the skin.

3.15. Ex Vivo Permeation Study. An ex vivo permeation study was performed to determine the ability of the DMN to permeate through rats' skin. The DMN permeation profiles of MP–MTF–GR (DMN2), MP–MTF (DMN2 without PBA), and pure MTF in four media are shown in Figure 7. After 24 h, the permeated MTF from pure MTF–DMN was 65.70 ± 2.63 , 63.81 ± 2.41 , 64.79 ± 2.79 , and 66.98 ± 1.16 μg for PBS, PBS + glucose 1%, PBS + glucose 2%, and PBS + glucose 4%, respectively. Furthermore, there was no significant difference ($p > 0.05$) in the permeated MTF in all media which indicated that the presence of glucose had no effect on the pure MTF permeation from DMN.

Interestingly, similar results were obtained for the permeated MTF from MP–MTF–DMN. After 24 h, the permeated MTF was 11.24 ± 0.55 , 11.48 ± 0.61 , 10.88 ± 1.47 , and 11.70 ± 0.67 μg from PBS, PBS + glucose 1%, PBS + glucose 2%, and PBS + glucose 4% media, respectively. There was no significant difference ($p > 0.05$) in the permeated MTF in all media, indicating that the presence of glucose also had no effect on MP–MTF permeation from DMN. However, the permeated MTF from MP–MTF–DMN was significantly lower ($p < 0.05$) than the permeated MTF from pure MTF–DMN in all media. When applied, DMN will form small pores as channels for the drug or drug MPs to pass through.²⁶ DMN-loaded drugs can deliver drugs directly; meanwhile, for drug MPs, it is necessary to pass through the polymer matrix first after being released from DMN.²³ This causes the MPs in the DMN to permeate less than the pure drug in the same time duration and provides longer MTF availability.

On the other hand, the MTF permeation from MP–MTF–GR–DMN obtained was 11.30 ± 0.29 , 23.31 ± 1.64 , 36.12 ± 3.77 , and 53.09 ± 3.01 μg from PBS, PBS + glucose 1%, PBS + glucose 2%, and PBS + glucose 4%, respectively. There was a significant increase ($p < 0.05$) in the permeated MTF with increasing glucose levels in the media. Accordingly, these results indicate that PBA as a GR material is not only successful in regulating the in vitro release of MTF but also able to regulate the ex vivo permeation of MTF based on the increase in glucose levels.

It is necessary to bear in mind that the dissolution time of DMN in the skin and the time required for MTF to be permeated entirely into the systemic tract were different. DMN

may be dissolved in 15 min, but the encapsulation system of MTF in the form of MPs can prolong the permeation time of MTF into the systemic tract. In addition, the GR material in the form of PBA linked to the polymer constituent of the MPs provides a permeation effect of MTF which is accelerated as the glucose level in the medium increases.¹⁸

In addition to considering the number of MTF successfully permeated, flux was also an important parameter in determining the profile and permeation behavior of MTF. Flux is defined as the number of drug molecules from the preparation that is able to permeate through a barrier in a certain time.^{49,50} The results of flux calculations from formulas DMN2, DMN2 without PBA, and pure MTF in various media are listed in Table 3. Based on the data, the highest flux was

Table 3. Flux Permeation of DMN2, DMN2 without PBA, and Pure MTF in PBA, PBS + Glucose 1%, PBS + Glucose 2%, and PBS + Glucose 4% Media (Mean \pm SD, $n = 3$)

media	flux at 24 h ($\mu\text{g}/\text{cm}^2/\text{h}$)		
	DMN2	DMN2 without PBA	pure MTF–DMN
PBS	0.871 ± 0.04	0.874 ± 0.06	7.534 ± 0.12
PBS + glucose 1%	2.122 ± 0.11	0.881 ± 0.07	7.614 ± 0.37
PBS + glucose 2%	3.301 ± 0.23	0.831 ± 0.08	7.630 ± 0.37
PBS + glucose 4%	4.974 ± 0.17	0.868 ± 0.06	7.869 ± 0.15

obtained in pure MTF and there was no significant difference ($p > 0.05$) in pure MTF flux in each medium. Meanwhile, the lowest flux was obtained in DMN2 without PBA ($p > 0.05$) and there were no significant differences between the media. DMN2 shows a decrease in flux than pure MTF, which shows a controlled release profile.⁵¹ The flux of DMN2 increased with increasing glucose levels in the medium, indicating that glucose levels affected the rate and MTF permeation profile of DMN2. This also proves that the presence of PBA in formula DMN2 could produce glucose-sensitive permeation behavior.

3.16. In Vivo Study in Diabetic Rats. To determine the effect of glucose control resulting from the formula, an in vivo study on diabetic rats was carried out (Figure 7E). The in vivo study was carried out on five groups of animals, namely, the healthy group (negative control), the diabetic group without treatment (positive control), the diabetic group that was given MTF orally, the diabetic group that was given DMN2, the diabetic group that was given DMN2 without PBA, and the diabetic group that was given pure MTF–DMN. The MTF oral group was given MTF at a dose of 100 mg/kg BW; meanwhile, all of the DMN groups were given six patches with a total MTF load of 453.48 μg . Diabetic induction was done by giving STZ injection. STZ injection causes glucose levels to exceed 400 mg/dL. In the positive diabetes group, a BGL of more than 400 mg/dL persisted until the end of the test. Meanwhile, in the healthy group, BGL was at normal levels (<200 mg/dL) and continued until the end of the test.

The MTF oral group was given MTF 100 mg/kg BW, and it showed a decrease in BGLs after 2 h of administration with a minimum BGL at 104.31 ± 11.47 mg/dL achieved after 3 h. MTF given orally could maintain glucose levels <200 mg/dL for up to 4 h. Meanwhile, the diabetic group given MTF–DMN showed a decrease in BGL that was achieved after 2 h and could be maintained for up to 3 h. The minimum BGL in the MTF–DMN group was 101.34 ± 9.12 mg/dL, achieved after 2 h. The diabetic group given DMN without PBA also

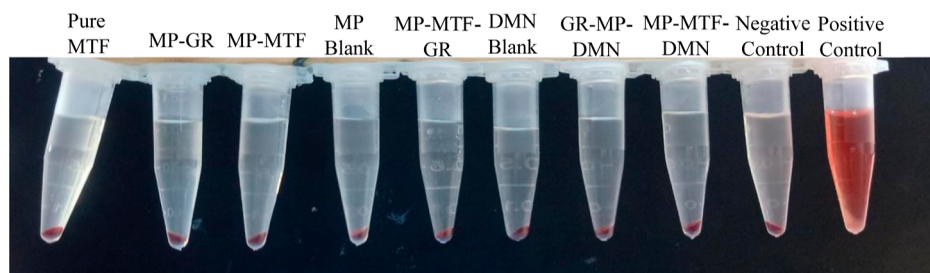


Figure 8. Hemolysis result of MP-MTF-GR, MP-MTF GR dissolvable MN, and their component prepared.

showed a decrease in normal glucose levels after 2 h with a minimum BGL of 104.34 ± 11.48 mg/dL. However, this formulation could produce a more prolonged glucose control effect (5 h) than oral MTF and pure MTF-DMN, indicating that the MP form could increase the prolonged MTF release. Hence, it could provide a longer glycemic effect.

The combination of MP-MTF-GR with DMN was able to produce better glucose control. In addition to the prolonged MTF effect of the MP form, the presence of a GR ingredient, namely, PBA, also produces a more controlled effect. PBA causes MTF to be more controlled according to glucose. The high BGL triggers the release of the MTF. The results of the glycemic control effect obtained were found to be longer. The administration of DMN2 produced a decrease in BGL after 3 h and maintained normal BGL for 8 h with a minimum BGL of 101.31 ± 11.28 mg/dL. This result indicated that the MP-MTF-GR-DMN formula was able to maintain normal BGL longer and better than oral MTF and other MTF-DMN formulas. In addition, when the PBA-glucose complex reached the equilibrium stage, PBA maintained its neutral form and no longer bound to glucose. The PBA reaction resulted in MTF no longer being released when glucose levels were normal and prevented hypoglycemic effects.⁵²

In the *in vivo* study, we evaluated the skin moisture of the rats. Water content of the skin is considered as one of the parameters of the skin barrier integrity.⁵³ Accordingly, in our study, we measured the skin moisture of the rats before and after the experiment. The results showed that the moisture content of the rats before the experiment was 71.43 ± 2.13 , 73.12 ± 3.53 , 74.29 ± 2.98 , 72.44 ± 2.78 , and $74.81 \pm 3.81\%$ for the healthy group, control group, oral group, DMN group with GR material, DMN group without GR material, and DMN group with pure MTF, respectively, indicating the normal skin condition of the rats. After the experiments, the respective groups showed skin moisture values of 72.65 ± 3.42 , 74.18 ± 2.76 , 72.09 ± 3.12 , 71.98 ± 3.41 , and $73.87 \pm 4.32\%$. Analyzed statistically, there were no significant differences ($p > 0.05$) in the skin moisture values in all rats. Therefore, skin integrity could be maintained during the experiment.

The result showed that the GR-MP-MTF-DMN formula can deliver MTF sufficiently to exert a glycemic control effect even with a reduced dose. Administration via DMN makes it possible to reduce the dose given because the DMN system could deliver drug particles efficiently to the systemic channel without losing the drug during the delivery.²⁰ However, these results need to be supported by pharmacokinetic data to determine the dose of loaded MTF in the formula and the size of the patch applied to the patient.

3.17. Hemolysis Test. The hemolysis test is an early-stage test conducted to determine the toxicity of newly developed pharmaceutical preparations. Hemolysis tests were carried out

on several samples to ensure that each material used was not potentially toxic to erythrocytes.²⁹

Here, we performed hemolysis tests on the active substance MTF, the compound that composes the MP, the compound that is GR, and the compound that composes the DMN (Figure 8). The test result showed that water as positive control causes hemolysis, which is indicated by the color of the test results that changes to red which indicates that the erythrocyte sample is lysed and mixed with water. Meanwhile, the PBS solution as negative control did not cause hemolysis which was indicated by the color of the solution that did not change. The same results were also obtained in all test samples. In addition, the calculation of the percentage of hemolysis in all samples obtained a value of less than 5%. It was found that all samples were not potentially toxic to erythrocytes.⁵⁴

Finally, in this research, a combination of GR-MP-MTF compounds was obtained, which is delivered through the optimal DMN system, which can deliver MTF efficiently and control its release with constituent compounds that are not toxic to the body's erythrocytes.

Overall, we successfully developed a selective delivery MP of MTF for specific delivery in the hyperglycemic condition. The formulations were able to release MTF based on the concentration of glucose in the media. This could be beneficial to avoid the possibility of hypoglycemia which could be caused by conventional oral administration. Furthermore, the incorporation of MP into DMN resulted in the formulation possessing adequate mechanical properties and insertion ability. Importantly, the *ex vivo* study showed the selective delivery of MPs through transdermal administration. In addition, the *in vivo* study showed the formula could decrease BGL in diabetic rats. Therefore, the combination approach developed in this study could potentially become alternative delivery to oral administration. To refine this concept, pharmacokinetic and pharmacodynamic studies are needed to determine the appropriate patch size given to the patient and the timing of subsequent use in multiple-dose administration. In chronic conditions like T2DM, it should be noted that the treatment would be done for a long period. Therefore, the deposition of polymers in the skin should be considered. Several studies show that PVP and PVA are biocompatible materials.^{55–57} Some studies focusing on the application of DMNs containing insulin have shown that the polymers were deposited in the skin.^{58,59} However, the deposition of the polymer following long-term and repeated application has not been studied. It has been suggested that to avoid the high deposition of the polymer in the skin following the application of DMNs, biodegradable polymers with low molecular weight could be used.⁵⁸ In this study, we used PVP and PVA such as PVP (K30) and PVA (10 kDa) with low molecular weight.

One of the critical points in the development of the DMN system is the translation of this technology. It has been suggested that a cooperative collaboration between industry and academia regarding the line scale-up production and manufacturing of DMNs, particularly in pharmacopoeial standards and good manufacturing practice (GMP) guidelines.⁶⁰ Additionally, the sterilization issue of products that will be inserted into the skin, such as DMNs, is undoubtedly something that needs to be considered. The holes formed from the administration of MNs can be a place for microbes to enter. However, this possibility returns to how deep and extensive the hole is. The gap created by MNs is much smaller than that produced by an injection needle (needs sterility); hence, recovery from the skin would be faster and the possibility of penetration of microbes into the skin is also much less. It was shown that even after repeated use on the skin, it did not interfere with the skin barrier function. In addition, the application of polymer-based MN formulas such as DMN and hydrogel-forming MN was found not to stimulate the humoral immune system.⁴³ Furthermore, it has been reported that the administration of MNs did not cause any microorganism penetration across the skin. Accordingly, it could be estimated that the risk of infection should not be caused by the administration of MN. However, further study is required to investigate the sterility of this combination approach.

With respect to the scaled-up manufacturing of this system, in this study, we used the micromolding method by utilizing centrifugation to remove bubbles and fill microholes perfectly. This method has proven to produce MNs with perfect physical shape. However, it is undeniable that this fabrication method has limitations for scaled-up manufacturing. Therefore, it is necessary to reconsider the fabrication method for scaled-up manufacturing. One promising method is the fabrication method in the form of a double-penetration female mold combined with the positive-pressure microperfusion technique (PPPT), showing that through this system, MNs can be produced in large quantities, with an optimal physical form.⁶¹ However, unfortunately, until now, there is still no official GMP standard for scale-up production from MNs. However, some previously marketed MN products, in reality, were not MNs but were described as very short hypodermic needles.⁶² Therefore, the absence of an official GMP standard is one of the significant obstacles, both in scaled-up manufacturing and distribution of MN products.

4. CONCLUSIONS

In this study, MTF was successfully developed in the form of MPs incorporated with a GR polymer using a combination of PBA and gelatin. The results of the physicochemical evaluation, including EE, particle size, and characterization with various instruments, including FTIR, DSC, and XRD, showed that MTF was completely entrapped in the PBA–gelatin polymer without changing its chemical structure. The in vitro release profile showed that this formula regulated the release of MTF dependent on glucose levels. Glucose-response-incorporated MTF MPs were also successfully delivered by dissolving MN with a combination of PVA and PVP as polymers. The results of the physicochemical evaluation of DMN showed adequate mechanical strength properties and penetration ability and stable DMN against environmental changes, including changes in humidity. The ex vivo permeation study of the developed formula shows permeation and release of MTF that occurs depending on

glucose levels. Importantly, the combination approach developed in this study showed a significant BGL in diabetic rats compared to other approaches. Thus, the combination of this system can be a solution as an alternative to MTF delivery to reduce gastrointestinal side effects and regulate the on-demand release of MTF, which depends on glucose levels to prevent the risk of hypoglycemia and increase the bioavailability of MTF. This system is promising to be further developed through in vivo testing and clinical testing to increase the therapeutic effect of MTF and reduce its adverse side effects to increase the effectiveness of T2DM therapy.

■ AUTHOR INFORMATION

Corresponding Author

Andi Dian Permana – Faculty of Pharmacy, Hasanuddin University, Makassar 90245, Indonesia; orcid.org/0000-0003-2168-1688; Email: andi.dian.permana@farmasi.unhas.ac.id

Authors

Nur Syafika – Faculty of Pharmacy, Hasanuddin University, Makassar 90245, Indonesia

Sumayya Binti Abdul Azis – Faculty of Pharmacy, Hasanuddin University, Makassar 90245, Indonesia

Cindy Kristina Enggi – Faculty of Pharmacy, Hasanuddin University, Makassar 90245, Indonesia

Hanin Azka Qonita – Faculty of Pharmacy, Hasanuddin University, Makassar 90245, Indonesia

Tiara Resky Anugrah Mahmud – Faculty of Medicine, Hasanuddin University, Makassar 90245, Indonesia

Ahmad Abizart – Faculty of Medicine, Hasanuddin University, Makassar 90245, Indonesia

Rangga Meidianto Asri – Faculty of Pharmacy, Hasanuddin University, Makassar 90245, Indonesia

Complete contact information is available at:

<https://pubs.acs.org/10.1021/acs.molpharmaceut.2c00936>

Author Contributions

The manuscript was written through contributions of all authors. All authors have given approval to the final version of the manuscript

Notes

The authors declare no competing financial interest.

■ ACKNOWLEDGMENTS

The authors thank Kementerian Pendidikan, Kebudayaan, Riset, dan Teknologi, and Hasanuddin University Indonesia for funding this study through the Program Kreativitas Mahasiswa (PKM).

■ LIST OF ABBREVIATIONS

BGL, blood glucose level; DL, drug loading; DM, diabetes mellitus; DMN, dissolving microneedle; DMSO, dimethyl sulfoxide; DSC, differential scanning calorimetry; EDC·HCl, 1-ethyl-3(3-dimethylaminopropyl) carbodiimide hydrochloride; EE, entrapment efficiency; FBG, fasting blood glucose; FTIR, Fourier transform infrared; GR, glucose response; MAA, moisture absorption ability; MN, microneedle; MP, microparticle; MP–MTF, microparticle metformin; MP–MTF–DMN, microparticle metformin–dissolvable microneedle; MP–MTF–GR, microparticle metformin–glucose response; MP–MTF–GR–DMN, microparticle metformin–glucose–

sponsive dissolvable microneedle; MTF, metformin; NHS, *N*-hydroxysuccinimide; PBA, phenylboronic acid; PBS, phosphate-buffered saline; PDI, polydispersity index; PVA, poly(vinyl alcohol); PVP, poly(vinyl pyrrolidone); SEM, scanning electron microscope; T2DM, type 2 diabetes mellitus; WVTR, water vapor transmission rate; XRD, X-ray diffraction

REFERENCES

- (1) International Diabetes Federation. *IDF Diabetes Atlas*, 10th ed.; International Diabetes Federation: Belgium, 2021.
- (2) Ghosal, S. The Side Effects Of Metformin—A Review. *J. Diabetes Metab. Disord.* **2019**, *6*, 030.
- (3) Ahmad, E.; Sargeant, J. A.; Zaccardi, F.; Khunti, K.; Webb, D. R.; Davies, M. J. Where Does Metformin Stand in Modern Day Management of Type 2 Diabetes? *Pharmaceuticals* **2020**, *13*, 427.
- (4) Baker, C.; Retzik-Stahr, C.; Singh, V.; Plomondon, R.; Anderson, V.; Rasouli, N. Should Metformin Remain the First-Line Therapy for Treatment of Type 2 Diabetes? *Ther. Adv. Endocrinol. Metab.* **2021**, *12*, 2042018820980225.
- (5) Migdadi, E. M.; Courtenay, A. J.; Tekko, I. A.; McCrudden, M. T. C.; Kearney, M. C.; McAlister, E.; McCarthy, H. O.; Donnelly, R. F. Hydrogel-Forming Microneedles Enhance Transdermal Delivery of Metformin Hydrochloride. *J. Controlled Release* **2018**, *285*, 142–151.
- (6) Wang, Y. W.; He, S. J.; Feng, X.; Cheng, J.; Luo, Y. T.; Tian, L.; Huang, Q. Metformin: A Review of Its Potential Indications. *Drug Des., Dev. Ther.* **2017**, *11*, 2421–2429.
- (7) Rena, G.; Hardie, D. G.; Pearson, E. R. The Mechanisms of Action of Metformin. *Diabetologia* **2017**, *60*, 1577–1585.
- (8) McCreight, L. J.; Bailey, C. J.; Pearson, E. R. Metformin and the Gastrointestinal Tract. *Diabetologia* **2016**, *59*, 426–435.
- (9) Spiller, H. A.; Quadrani, D. A. Toxic Effects from Metformin Exposure. *Ann. Pharmacother.* **2004**, *38*, 776–780.
- (10) Aldobeaban, S.; Mzahim, B.; Alshehri, A. A. Recurrent Hypoglycemia Secondary to Metformin Toxicity in the Absence of Co-Ingestions: A Case Report. *J. Med. Case Rep.* **2018**, *12*, 223.
- (11) Liu, T.; Jiang, G.; Song, G.; Zhu, J.; Yang, Y. Fabrication of Separable Microneedles with Phase Change Coating for NIR-Triggered Transdermal Delivery of Metformin on Diabetic Rats. *Biomed. Microdevices* **2020**, *22*, 12.
- (12) Liu, J. F.; Bian, J.; Issadore, D.; Tsourkas, A. Use of Magnetic Fields and Nanoparticles to Trigger Drug Release and Improve Tumor Targeting. *Wiley Interdiscip. Rev.: Nanomed. Nanobiotechnol.* **2020**, *11*, 1571.
- (13) Wu, J.; Williams, G. R.; Li, H.; Wang, D.; Li, S.; Zhu, L.-M. Insulin-Loaded PLGA Microspheres for Glucose-Responsive Release. *Drug Delivery* **2017**, *24*, 1513–1525.
- (14) Kubota, T.; Kurashina, Y.; Zhao, J.; Ando, K.; Onoe, H. Ultrasound-Triggered on-Demand Drug Delivery Using Hydrogel Microbeads with Release Enhancer. *Mater. Des.* **2021**, *203*, 109580.
- (15) Ma, Q.; Zhao, X.; Shi, A.; Wu, J. Bioresponsive Functional Phenylboronic Acid-Based Delivery System as an Emerging Platform for Diabetic Therapy. *Int. J. Nanomed.* **2021**, *16*, 297–314.
- (16) Shen, D.; Yu, H.; Wang, L.; Chen, X.; Feng, J.; Zhang, Q.; Xiong, W.; Pan, J.; Han, Y.; Liu, X. Biodegradable Phenylboronic Acid-Modified ϵ -Polylysine for Glucose-Responsive Insulin Delivery via Transdermal Microneedles. *J. Mater. Chem. B* **2021**, *9*, 6017–6028.
- (17) Wang, X.; Wei, B.; Cheng, X.; Wang, J.; Tang, R. Phenylboronic Acid-Decorated Gelatin Nanoparticles for Enhanced Tumor Targeting and Penetration. *Nanotechnology* **2016**, *27*, 385101.
- (18) Gupta, M. K.; Prakash, D.; Mishra, B. Biodegradable Microparticulate Drug Delivery System of Diltiazem HCl. *Braz. J. Pharm. Sci.* **2012**, *48*, 699–709.
- (19) Lengyel, M.; Kállai-Szabó, N.; Antal, V.; Laki, A. J.; Antal, I. Microparticles, Microspheres, and Microcapsules for Advanced Drug Delivery. *Sci. Pharm.* **2019**, *87*, 20.
- (20) Waghule, T.; Singhvi, G.; Dubey, S. K.; Pandey, M. M.; Gupta, G.; Singh, M.; Dua, K. Microneedles: A smart approach and increasing potential for transdermal drug delivery system. *Biomed. Pharmacother.* **2019**, *109*, 1249–1258.
- (21) Permana, A. D.; Tekko, I. A.; McCrudden, M. T. C.; Anjani, Q. K.; Ramadan, D.; McCarthy, H. O.; Donnelly, R. F. Solid Lipid Nanoparticle-Based Dissolving Microneedles: A Promising Intradermal Lymph Targeting Drug Delivery System with Potential for Enhanced Treatment of Lymphatic Filariasis. *J. Controlled Release* **2019**, *316*, 34–52.
- (22) Al-japairai, K. A. S.; Mahmood, S.; Almurisi, S. H.; Venugopal, J. R.; Hilles, A. R.; Azmana, M.; Raman, S. Current Trends in Polymer Microneedle for Transdermal Drug Delivery. *Int. J. Pharm.* **2020**, *587*, 119673.
- (23) He, J.; Zhang, Z.; Zheng, X.; Li, L.; Qi, J.; Wu, W.; Lu, Y. Design and Evaluation of Dissolving Microneedles for Enhanced Dermal Delivery of Propranolol Hydrochloride. *Pharmaceutics* **2021**, *13*, 579.
- (24) Volpatti, L. R.; Matranga, M. A.; Cortinas, A. B.; Delcassian, D.; Daniel, K. B.; Langer, R.; Anderson, D. G. Glucose-Responsive Nanoparticles for Rapid and Extended Self-Regulated Insulin Delivery. *ACS Nano* **2020**, *14*, 488–497.
- (25) Danaei, M.; Dehghankhold, M.; Ataei, S.; Hasanzadeh Davarani, F.; Javanmard, R.; Dokhani, A.; Khorasani, S.; Mozafari, M. R. Impact of Particle Size and Polydispersity Index on the Clinical Applications of Lipidic Nanocarrier Systems. *Pharmaceutics* **2018**, *10*, 57.
- (26) Permana, A. D.; Paredes, A. J.; Volpe-Zanutto, F.; Anjani, Q. K.; Utomo, E.; Donnelly, R. F. Dissolving Microneedle-Mediated Dermal Delivery of Itraconazole Nanocrystals for Improved Treatment of Cutaneous Candidiasis. *Eur. J. Pharm. Biopharm.* **2020**, *154*, 50–61.
- (27) Yu, J.; Wang, J.; Zhang, Y.; Chen, G.; Mao, W.; Ye, Y.; Kahkoska, A. R.; Buse, J. B.; Langer, R.; Gu, Z. Glucose-Responsive Insulin Patch for the Regulation of Blood Glucose in Mice and Minipigs. *Nat. Biomed. Eng.* **2020**, *4*, 499–506.
- (28) Larrañeta, E.; Moore, J.; Vicente-Pérez, E. M.; González-Vázquez, P.; Lutton, R.; Woolfson, A. D.; Donnelly, R. F. A Proposed Model Membrane and Test Method for Microneedle Insertion Studies. *Int. J. Pharm.* **2014**, *472*, 65–73.
- (29) Ananda, P. W. R.; Elim, D.; Zaman, H. S.; Muslimin, W.; Tunggeng, M. G. R.; Permana, A. D. Combination of Transdermal Patches and Solid Microneedles for Improved Transdermal Delivery of Primaquine. *Int. J. Pharm.* **2021**, *609*, 121204.
- (30) Cheng, A.; Sun, W.; Xing, M.; Zhang, S.; Gao, Y. The Hygroscopicity of Polymer Microneedles on the Performance of Dissolving Behavior for Transdermal Delivery. *Int. J. Polym. Mater. Polym. Biomater.* **2022**, *71*, 72–78.
- (31) Farris, S.; Song, J.; Huang, Q. Alternative Reaction Mechanism for the Cross-Linking of Gelatin with Glutaraldehyde. *J. Agric. Food Chem.* **2010**, *58*, 998–1003.
- (32) *Encyclopedia of Membranes*; Drioli, E.; Giorno, L., Eds; Springer, 2016.
- (33) Jyothi, N. V. N.; Prasanna, P. M.; Sakarkar, S. N.; Prabha, K. S.; Ramaiah, P. S.; Srawan, G. Y. Microencapsulation Techniques, Factors Influencing Encapsulation Efficiency. *J. Microencapsulation* **2010**, *27*, 187–197.
- (34) Liu, Y.; Yang, G.; Jin, S.; Xu, L.; Zhao, C.-X. Development of High-Drug-Loading Nanoparticles. *ChemPlusChem* **2020**, *85*, 2143–2157.
- (35) Gabel, S. A.; Duff, M. R.; Pedersen, L. C.; DeRose, E. F.; Krahn, J. M.; Howell, E. E.; London, R. E. A Structural Basis for Biguanide Activity. *Biochemistry* **2017**, *56*, 4786.
- (36) Bouriche, S.; Alonso-García, A. A.; Cárceles-Rodríguez, C. M. C.; Rezugui, F.; Fernández-Varón, E. F. An in Vivo Pharmacokinetic Study of Metformin Microparticles as an Oral Sustained Release Formulation in Rabbits. *BMC Vet. Res.* **2021**, *17*, 315.
- (37) Adamczyk-Woźniak, A.; Gozdalik, J. T.; Kaczorowska, E.; Durka, K.; Wiczorek, D.; Zarzeckańska, D.; Sporyński, A. (Trifluoromethoxy)Phenylboronic Acids: Structures, Properties, and Antibacterial Activity. *Molecules* **2021**, *26*, 2007.

- (38) Foox, M.; Zilberman, M. Drug Delivery from Gelatin-Based Systems. *Expert Opin. Drug Delivery* **2015**, *12*, 1547–1563.
- (39) Zhao, L.; Huang, Q.; Liu, Y.; Wang, Q.; Wang, L.; Xiao, S.; Bi, F.; Ding, J. Boronic Acid as Glucose-Sensitive Agent Regulates Drug Delivery for Diabetes Treatment. *Materials (Basel)* **2017**, *10*, 170.
- (40) Bruschi, M. L. Mathematics Model of Drug Release. *Strategies to Modify the Drug Release from Pharmaceutical Systems*; Woodhead Publishing, 2015; pp 63–86.
- (41) Shim, W. S.; Hwang, Y. M.; Park, S. G.; Lee, C. K.; Kang, N. G. Role of Polyvinylpyrrolidone in Dissolving Microneedle for Efficient Transdermal Drug Delivery: In Vitro and Clinical Studies. *Bull. Korean Chem. Soc.* **2018**, *39*, 789–793.
- (42) Zhu, Z.; Luo, H.; Lu, W.; Luan, H.; Wu, Y.; Luo, J.; Wang, Y.; Pi, J.; Lim, C. Y.; Wang, H. Rapidly Dissolvable Microneedle Patches for Transdermal Delivery of Exenatide. *Pharm. Res.* **2014**, *31*, 3348–3360.
- (43) Vicente-Pérez, E. M.; Quinn, H. L.; McAlister, E.; O'Neill, S.; Hanna, L. A.; Barry, J. G.; Donnelly, R. F. The Use of a Pressure-Indicating Sensor Film to Provide Feedback upon Hydrogel-Forming Microneedle Array Self-Application in Vivo. *Pharm. Res.* **2016**, *33*, 3072–3080.
- (44) International Council for Harmonisation. Technical Requirements for Registration of Pharmaceuticals for Human Use: The ICH Process. *The Textbook of Pharmaceutical Medicine*; Wiley, 2005; p 447.
- (45) Proksch, E. PH in Nature, Humans and Skin. *J. Dermatol.* **2018**, *45*, 1044–1052.
- (46) Zhang, K.; Yu, Q.; Zhu, L.; Liu, S.; Chi, Z.; Chen, X.; Zhang, Y.; Xu, J. The Preparations and Water Vapor Barrier Properties of Polyimide Films Containing Amide Moieties. *Polymers (Basel)* **2017**, *9*, 677.
- (47) Singh, A.; Bali, A. Formulation and Characterization of Transdermal Patches for Controlled Delivery of Duloxetine Hydrochloride. *J. Anal. Sci. Technol.* **2016**, *7*, 25.
- (48) Wang, Q. L.; Ren, J. W.; Chen, B. Z.; Jin, X.; Zhang, C. Y.; Guo, X. D. Effect of Humidity on Mechanical Properties of Dissolving Microneedles for Transdermal Drug Delivery. *J. Ind. Eng. Chem.* **2018**, *59*, 251–258.
- (49) Elshall, A. A.; Ghoneim, A. M.; Abdel-Mageed, H. M.; Osman, R.; Shaker, D. S. Ex Vivo Permeation Parameters and Skin Deposition of Melatonin-Loaded Microemulsion for Treatment of Alopecia. *Future J. Pharm. Sci.* **2022**, *8*, 28.
- (50) Silva-Abreu, M.; Espinoza, L. C.; Halbaut, L.; Espina, M.; García, M. L.; Calpena, A. C. Comparative Study of Ex Vivo Transmucosal Permeation of Pioglitazone Nanoparticles for the Treatment of Alzheimer's Disease. *Polymers (Basel)* **2018**, *10*, 316.
- (51) Rao, M. T.; Rao, Y. S.; Ratna J, J.; Kumari Pv, P. V. Characterization and Ex Vivo Studies of Nanoparticle Incorporated Transdermal Patch of Itraconazole. *Indian J. Pharm. Sci.* **2020**, *82*, 799–808.
- (52) Elshaarani, T.; Yu, H.; Wang, L.; Zain-ul-Abdin, Z.; Ullah, R. S.; Haroon, M.; Khan, R. U.; Fahad, S.; Khan, A.; Nazir, A.; Usman, M.; Naveed, K. U. R. Synthesis of hydrogel-bearing phenylboronic acid moieties and their applications in glucose sensing and insulin delivery. *J. Mater. Chem. B* **2018**, *6*, 3831.
- (53) Chirikhina, E.; Chirikhin, A.; Xiao, P.; Dewsbury-Ennis, S.; Bianconi, F. In Vivo Assessment of Water Content, Trans-Epidermal Water Loss and Thickness in Human Facial Skin. *Appl. Sci.* **2020**, *10*, 6139.
- (54) Zhou, H. Y.; Zhang, Y. P.; Zhang, W. F.; Chen, X. G. Biocompatibility and Characteristics of Injectable Chitosan-Based Thermosensitive Hydrogel for Drug Delivery. *Carbohydr. Polym.* **2011**, *83*, 1643–1651.
- (55) El-Houssiny, A. S.; Ward, A. A. M.; Mansour, S. H.; Abd-El-Messieh, S. L. Biodegradable Blends Based on Polyvinyl Pyrrolidone for Insulation Purposes. *J. Appl. Polym. Sci.* **2012**, *124*, 3879–3891.
- (56) Franco, P.; De Marco, I. The Use of Poly(N-Vinyl Pyrrolidone) in the Delivery of Drugs: A Review. *Polymers (Basel)* **2020**, *12*, 1114.
- (57) Ben Halima, N. Poly(Vinyl Alcohol): Review of Its Promising Applications and Insights into Biodegradation. *RSC Adv.* **2016**, *6*, 39823–39832.
- (58) McAlister, E.; Kirkby, M.; Domínguez-Robles, J.; Paredes, A. J.; Anjani, Q. K.; Moffatt, K.; Vora, L. K.; Hutton, A. R. J.; McKenna, P. E.; Larrañeta, E.; Donnelly, R. F. The Role of Microneedle Arrays in Drug Delivery and Patient Monitoring to Prevent Diabetes Induced Fibrosis. *Adv. Drug Delivery Rev.* **2021**, *175*, 113825.
- (59) Ito, Y.; Hirono, M.; Fukushima, K.; Sugioka, N.; Takada, K. Two-Layered Dissolving Microneedles Formulated with Intermediate-Acting Insulin. *Int. J. Pharm.* **2012**, *436*, 387–393.
- (60) Indermun, S.; Luttgge, R.; Choonara, Y. E.; Kumar, P.; du Toit, L. C.; Modi, G.; Pillay, V. Current Advances in the Fabrication of Microneedles for Transdermal Delivery. *J. Controlled Release* **2014**, *185*, 130–138.
- (61) Chen, H.; Wu, B.; Zhang, M.; Yang, P.; Yang, B.; Qin, W.; Wang, Q.; Wen, X.; Chen, M.; Quan, G.; Pan, X.; Wu, C. A Novel Scalable Fabrication Process for the Production of Dissolving Microneedle Arrays. *Drug Delivery Transl. Res.* **2019**, *9*, 240–248.
- (62) Lutton, R. E. M.; Moore, J.; Larrañeta, E.; Liggett, S.; Woolfson, A. D.; Donnelly, R. F. Microneedle Characterisation: The Need for Universal Acceptance Criteria and GMP Specifications When Moving towards Commercialisation. *Drug Delivery Transl. Res.* **2015**, *5*, 313–331.

Recommended by ACS

Compound Nanoemulsion Combined with Differentiation/Cytotoxicity Drugs for Modulating Breast Cancer Stemness

Yongchao Chu, Tao Sun, *et al.*

JANUARY 30, 2023
MOLECULAR PHARMACEUTICS

READ 

Analysis of Cimetidine Crystal Polymorphs by X-ray Absorption Near-Edge Spectroscopy

Hironori Suzuki, Shuji Noguchi, *et al.*

DECEMBER 23, 2022
MOLECULAR PHARMACEUTICS

READ 

Reliable Kinetics for Drug Delivery with a Microfluidic Device Integrated with the Dialysis Bag

Javad Esmaeili, Jafar Ai, *et al.*

JANUARY 18, 2023
MOLECULAR PHARMACEUTICS

READ 

Hybrid Micelles of Carbon Quantum Dot–Doxorubicin Conjugates as Nanotheranostics for Tumor Therapy and Turn-On Fluorescence Imaging: Impact of Conjugated St...

Jie Li, Peng Liu, *et al.*

JANUARY 23, 2023
MOLECULAR PHARMACEUTICS

READ 

Get More Suggestions >